The Role of Deubiquitinating Enzyme USP22 in Human Somatic Cell Reprogramming

by

Gülben Gürhan

A Dissertation Submitted to the
Graduate School of Health Sciences in Partial
Fulfillment of the Requirements for the Degree
of

Doctor of Philosophy

in

Cellular and Molecular Medicine

KOÇ ÜNİVERSİTESİ

May 30, 2023

The Role of Deubiquitinating Enzyme USP22 in Human Somatic Cell Reprogramming

Koc University

Graduate School of Health Sciences

This is to certify that I have examined this copy of a doctoral dissertation by

Gülben Gürhan

and have found that it is complete and satisfactory in all respects,
and that any and all revisions required by the final
examining committee have been made.

Committee Members:

Prof. Tamer Önder (Advisor)

Asst. Prof. Gözde Korkmaz

Assoc. Prof. NC Tolga Emre

Asst. Prof. Ece Öztürk

Prof. Batu Erman

Date: 30/05/2023

To the most special women in my life; my mother and daughter...

ABSTRACT

The Role of Deubiquitinating Enzyme USP22 in Human Somatic Cell Reprogramming

Gülben Gürhan

Doctor of Philosophy in Cellular and Molecular Medicine May 30, 2023

Human somatic cells can be reprogrammed to induced pluripotent stem cells (iPSC) by overexpressing OCT4, SOX2, KLF4 and MYC (OSKM). There are cell intrinsic barriers to reprogramming. We conducted a CRISPR-Cas9-mediated knockout screen during reprogramming to reveal chromatin pathways acting as barriers to reprogramming. Other than DNMT3A and EP300 which were already known to be barriers to reprogramming, this screen revealed a barrier role for USP22 during reprogramming. In this thesis, I validated the barrier role of USP22 in reprogramming by loss-of-function assay. In addition to this, overexpression of various USP22 mutants revealed that USP22 deubiquitinase activity or its integration into the SAGA complex does not affect reprogramming. Interestingly, CRISPR-Cas9-mediated knockout of SAGA deubiquitinase members, ATXN7L3 and ENY2 had no positive impact on reprogramming efficiency. To investigate the effect of USP22 on human pluripotency, I obtained single USP22 knockout clones. These clones expressed pluripotency markers, contributed to tissues from three germ layers when subjected to teratoma formation assay and showed normal karyotyping as in control pluripotent stem cells. To understand the defects in specific lineage specifications, these clones were subjected to in vitro embryoid body formation assay. There seem problems in pluripotency exit as revealed by unsuccessful downregulation of pluripotency markers such as OCT4 and SOX2. Furthermore, mesoderm and endoderm differentiation defects were observed in one of USP22 knockout clones compared to wild-type clones as judged by the lower expression levels of marker genes. To gain more mechanistic insight on the USP22 loss-mediated enhanced reprogramming, we performed an RNA-Seq experiment. USP22 knockout and wild-type fibroblasts were reprogrammed by OSKM expression and on day 6 of reprogramming RNA-Seq was performed. Expectedly, we observed that development-related genesets were negatively enriched whereas pluripotency-related genesets were positively enriched by USP22 loss. SOX2 target geneset was among positively enriched genesets and we hypothesized that USP22 loss activates endogenous pluripotency network earlier during reprogramming to increase its efficiency. To test this hypothesis, we collected RNA at different days of reprogramming and revealed that endogenous SOX2 levels increased up to 3-fold upon USP22 loss during reprogramming. These results show that USP22 acts as a barrier to reprogramming by suppressing endogenous pluripotency network independent from its catalytic activity and SAGA incorporation.

OZETCE

İnsan Somatik Hücre Yeniden Programlamasında Deubiquitinating Enzim USP22'nin Rolü

Gülben Gürhan, Doktora

30 Mayıs 2023

OCT4, SOX2, KLF4 ve MYC (OSKM) anlatımıyla insan somatik hücreleri indüklenmiş pluripotent kök hücrelere (iPKH) yeniden programlanabilir. Yeniden programlamaya engel hücre içi mekanizmalar mevcuttur. Kromatin yolaklarından yeniden programlamaya engel olacakları bulmak için CRISPR-Cas9 ile susturma taraması yaptık. DNMT3A ve EP300 gibi yeniden programlamaya bariyer olduğu bilinen genlerin dışında bu tarama USP22 için de bariyer rol belirlemiştir. Bu tezde fonksiyon kaybı yöntemiyle USP22'nin bariyer rolü teyit edilmiştir. Bunun üstüne, USP22'nin farklı mutantlarının anlatımıyla, USP22'nin katalitik aktivitesinin ve SAGA kompleksine katılımının yeniden programlama üzerinde bir etkisi olmadığı ortaya çıkmıştır. İlgi çekici olarak, ATXN7L3 ve ENY2 gibi SAGA DUB modülüne ait genler CRISPR-Cas9 metoduyla susturulduğunda, yeniden programlama verimi üzerinde herhangi bir olumlu etkisi görülmemiştir. USP22'nin insan pluripotensisi üzerindeki etkisini araştırmak için USP22 geni susturulmuş tek hücreden büyüyen klonlar elde edilmiştir. Bu klonlar tıpkı kontrol klonları gibi pluripotensi belirteçlerinin anlatımını sağlamış, teratom oluştururken üç embriyonik tabakadan dokulara farklılaşabilmiş ve normal karyotip göstermişlerdir. Belirli tabakalara farklılaşmadaki hataları anlamak için bu klonlar in vitro farklılaşmaya maruz bırakılmışlardır. OCT4 ve SOX2 gibi pluripotensi belirteçlerinin basarisiz bir şekilde düşmesiyle, plurpotensiden çıkışta problemler saptanmıştır. Dahası, mezoderm ve endoderm farklılaşmada USP22 susturulmuş klonlarda belirteçlerin daha düşük anlatımı olduğu için problemler saptanmıştır. USP22'nin susturulmasıyla artan yeniden programlama verimi hakkında daha mekanistik bilgi kazanmak için RNA-dizileme yapılmıştır. USP22 geni susturulmuş ve kontrol fibroblastlar OSKM anlatımıyla yeniden programlanmış ve 6. günde RNA-dizileme yapılmıştır. Beklendiği üzere, gelişim ile ilgili gen setleri USP22'nin silinmesiyle negatife korele olurken pluripotensi ile ilgili gen setleri pozitif korele olmuştur. SOX2 hedef genleri pozitif korele olan gen setlerinden biriydi ve biz USP22'nin silinmesiyle endojen pluripotensi ağı yeniden programlamada daha erken aktive olarak verimi arttırmaktadır diye hipotez geliştirdik. Bu hipotezi test etmek için yeniden programlamanın farklı günlerinde RNA toplanarak endojen SOX2 seviyesinin kontrole göre 3 kata kadar arttığı gösterilmiştir. Bu sonuçlar USP22'nin endojen plurpotensi ağını katalitik aktivitesi ve SAGA'dan bağımsız olarak baskılayarak yeniden programlamaya engel olduğunu göstermiştir.

ACKNOWLEDGMENTS

First, I would like to thank my esteemed thesis advisor, Tamer Önder, for all the opportunities he provided me in my scientific adventure, which started as a technician in his laboratory. During my Ph.D., he enthusiastically supported my life, which was utterly transformed, and did not make it a priority that it could affect my work.

After my thesis advisor, I would like to thank Can Aztekin first. It is very valuable to me that you warded off all the loss of self-confidence I experienced by hitting my head and that you continue to do so. The "GG" pattern you added to my life is still very trendy, like our mini-prep memories. I learned how to be a true scientist discipline from you, little brother.
A very late thank you to Ayyub Ebrahimi and Kerem Fidan. For contributing to my technical development by sharing everything they know and the warm friendship environment they provided me while I was trying to adapt here.

I would also like to thank my friend Mert Gayretli for what he has done so far and will do in the future. You added fun to my life during the most stressful times of the thesis, my friend.

Özge&Eren, and my little bird Bilge, the new member of the Şahin family, your presence and even missing you add a lot of meaning to my life. What other friend could have shown such understanding to the doctoral thesis that came between us?

Finally in my life, "we tried even if we got crazy ideas and failed!" There is one person I can call. I would like to thank Alperen Yılmaz for standing firm like a huge plane tree against the whole world and supporting me with all your might during this period when I was trying to rebuild my life and my thesis project. The things you have contributed to this project intellectually cannot be underestimated. Being a scientist suits you very well, cool boy of the lab. More great fantastic projects...

The most powerful and valuable person in my life, my dear mother, Nuray Gürhan, you're teaching me to deal with difficulties like you and never give up, made this thesis exist.
My dear father Hayrettin Gürhan, it was very valuable to feel that you trust me until now. I will carry the vision you instilled in me as a child on my chest like a medal for the rest of my life.

My dear mother-in-law and father-in-law Ayten Sevinç and Metin Sevinç, thank you very much for making my life easier by looking after my dear daughter Maya, who was the craziest decision of my life, despite all the difficulties during my Ph.D.

I would also like to thank my very precious spiritual aunt Şenay Durmaz, her precious husband İsmail Durmaz, and their daughters Buket and Nil for the warm home they provided me and my daughter during the writing of the thesis.

Yes, you are next, my life partner Kenan Sevinç. It has been a very instructive experience to collaborate with you on so many projects, experiments, and our nuclear family throughout this entire process. Thank you for encouraging me to do things I didn't dare bring into my life.

Finally, thank you very much, my dear daughter, Maya for teaching me again how to ask thousands of questions to the universe through the eyes of a child, and for reminding me why I chose this path, and that the simplest questions are the most curious ones. I love you my cute little witch.

TABLE OF CONTENTS

LIST OF TABLES

LIST OF FIGURES

ABBREVIATIONS

ICM	Inner cell mass
TSC	Trophoblast stem cell
ESC	Embryonic stem cell
PGC	Primordial germ cell
TF	Transcription factor
OSKM	Oct4, Sox2, Klf4 and c-Myc
iPSC	Induced pluripotent stem cells
MEF	Mouse embryonic fibroblast
MET	Mesenchymal-to-epithelial transition
EMT	Epithelial-to-mesenchymal transition
SAGA	SPT-ADA-GCN5 acetylase
USP22	Ubiquitin specific peptidase 22
DMSO	Dimethyl sulfoxide protein
EP300, p300	E1A binding protein p300
BRD9	Bromodomain containing-9
PRC	Polycomb repressive complex
CRISPR	Clustered Regularly Interspaced Short Palindromic Repeats
GSEA	Gene set enrichment analysis
ChIP	Chromatin immunoprecipitation
GO	Gene Ontology
DNMT	DNA (cytosine-5)-methyltransferase
HAT	Histone acetyltransferase
DMEM	Dulbecco's Modified Eagle Medium
PBS	Phosphate-buffered saline
KO	Knock-out
RT qPCR	Real time quantitative polymerase chain reaction
cDNA	Complementary DNA
Ct	Threshold cycle
IVF	In vitro fertilization
TE	Trophoectoderm
ECCs	Embryonic carcinoma cell
ALS	Amyotrophic lateral sclerosis
SMA	Spinal muscular atrophy

PSC	Pluripotent stem cell
HDAC	Histone deacetylase
SAHA	Suberoylanilide hydroxamic acid
TSA	Trichostatin A
VPA	Valproic acid
DUB	Deubiquitination
NHDF	Normal human dermal fibroblast

Chapter 1

INTRODUCTION

1.1. Embryonic stem cells and pluripotency

Embryonic stem cells (ESCs) are a type of stem cell that are derived from the inner cell mass of a developing embryo (Cowan et al., 2004; Evans & Kaufman, 1981; Klimanskaya et al., 2006; Martin, 1981; Thomson et al., 1998). They can differentiate into any type of cell in the body which is a property known as pluripotency (Oh & Jang, 2019). During embryonic development, stem cells possessing this "pluripotent" state differentiate into three germ layers, the endoderm, mesoderm and ectoderm, eventually giving rise to all of the tissues and organs in the adult organism(Romito & Cobellis, 2016). Due to this concept, capturing these pluripotent cells in the dish can provide valuable tools for studying different aspects of development and disease modeling. Their high differentiation capability can be leveraged in regenerative medicine by creating replacement tissues for lost or damaged tissues. However, a major drawback that prevented the use of pluripotent stem cells in research and therapy was the source of these cells. Embryonic stem cells (ESCs) which were initially the only pluripotent stem cell type available are derived by destroying embryos thereby limiting the use of pluripotent stem cells due to ethical concerns (Cowan et al., 2004). To bypass these issues, alternative ways to generate pluripotent stem cells have been developed.

1.2. From pre-implantation to cellular reprogramming

Pre-implantation refers to the early stage of embryonic development that occurs prior to implantation of the embryo in the uterus. This stage begins with fertilization, when the sperm and egg form a single-cell zygote, and continues through several rounds of cell division, resulting in a small cluster of cells called a blastocyst (Leung & Zernicka-Goetz, 2015; Molè et al., 2020; M. Zhu & Zernicka-Goetz, 2020). During pre-implantation, the developing embryo undergoes a series of critical developmental milestones, including the formation of the blastocyst, the establishment of embryonic polarity, and the initiation of cell differentiation (Leung & Zernicka-Goetz, 2015). These milestones are essential for the proper development of the embryo and its subsequent implantation and growth in the uterus.

The first lineage specification takes place at the blastula stage during development (Jedrusik, 2015). Inner cells of blastocyst turn into inner cell mass (ICM) and outer cells make extra-embryonic lineage called trophectoderm (TE) during this stage (Jedrusik, 2015). There are certain factors necessary for generating and maintaining this cell fate decision. For example, inhibition of the Hippo pathway upregulates Cdx2 to maintain TE lineage identity and key transcription factors such as Cdx2 and Eomes define TE cell identity (M. Zhu & Zernicka-Goetz, 2020). On the other hand, the co-occupancy of Oct4, Sox2 and Nanog in the inner cells' genome defines an ICM fate and Oct4-mediated Cdx2 downregulation maintains ICM lineage cell identity (Jedrusik, 2015).

Pre-implantation embryos can be used in a number of research applications, including genetic screening and analysis, stem cell research, and the development of new reproductive technologies. In some cases, pre-implantation embryos may also be used in assisted reproduction techniques, such as in vitro fertilization (IVF), to help individuals and couples achieve pregnancy.

Differentiation was thought to be a one-way process resulting in a cell identity proposed to be strictly conserved in adulthood as proposed by Waddington's epigenetic landscape (Waddington, 1956). However, this hypothesis was challenged by several observations over the following decades. Dr. John Gurdon, in a landmark paper in 1962, showed that if the nucleus of a somatic cell is transferred into an enucleated Xenopus oocyte, it can generate a mature frog (FISCHBERG et al., 1958; GURDON, 1960, 1962b, 1962a). Moreover, differentiated cells dedifferentiate to gain a pluripotent character if they are fused with a pluripotent stem cell such as ESCs, embryonic carcinoma cells (ECCs) and primordial germ cells (PGCs) (Cowan et al., 2005; Do & Schöler, 2006; Tada et al., 1997, 2001). Lastly, cellular identity can be altered by overexpressing lineage-specific transcription factors (TFs). The first example of this type of conversion was demonstrated through overexpressing MyoD, a muscle cell-specific transcription factor, which led to the trans-differentiation of mouse fibroblasts to myoblasts (Choi et al., 1990). Later studies proved that expression of specific transcription factors can mediate other types of lineage-conversions, showing that cells can be "reprogrammed" to acquire different identities (Duran Alonso et al., 2018; Ieda, 2013; M. Wang et al., 2019; H. Zhu et al., 2020). These experiments demonstrated that Waddington's epigenetic landscape can be traversed in multiple directions with cells being able to acquire new identities or moving "up" to a higher state of potency.

Cellular reprogramming involves taking an already differentiated cell, such as a skin fibroblast cell, and reprogramming it back into a pluripotent state. This is typically done by

introducing specific transcription factors that regulate gene expression and can "turn back the clock" on the cell, effectively erasing its specialized identity and returning it to a more primitive state (Brumbaugh et al., 2019; Hanna et al., 2008). The first successful reprogramming of cells was done using mouse fibroblasts in 2006, and the technique was later adapted for use with human cells (K. Takahashi et al., 2007; K. Takahashi & Yamanaka, 2006). The resulting cells are called induced pluripotent stem cells (iPSCs) and have many of the same properties as embryonic stem cells, including pluripotency. Somatic cells can be reprogrammed to induced pluripotent stem cells (iPSCs) by overexpressing OCT4, SOX2, KLF4 and c-MYC (OSKM) transcription factors. This dedifferentiation protocol takes approximately 3 weeks for human iPSC colony generation. During the initial period of this process, somatic transcription program turns off and mesenchymal-to-epithelial transition occurs (Hanna et al., 2008; Pei et al., 2019). Towards the end of reprogramming, endogenous pluripotency transcription network is activated and emerging iPSCs become transgene independent (Papp & Plath, 2011). Moreover, iPSCs display ESC-like properties such as self-renewal and capability to differentiate into three germ layers. Interestingly, reprogramming efficiency from human adult fibroblasts, as defined by the number of iPSC generated per input somatic cells, is lower than 1%, even when OSKM are provided to each cell at high copy number (Park et al., 2008; K. Takahashi et al., 2007; Y. Wang et al., 2018). This observation suggested that there are intrinsic barriers for reprogramming that delay either the repression of somatic programs or the activation of the pluripotency network. There are also several other potential cell-intrinsic processes that block reprogramming such as cell cycle regulators, senescence and apoptosis (Aarts et al., 2017; E. J. Y. Kim et al., 2018; Rand et al., 2018; Tran et al., 2019; Y. Wang, Chen, et al., 2020).

The ability to reprogram cells has opened up new avenues of research and holds great promise for regenerative medicine. It may be possible to use iPSCs to replace damaged or diseased cells, or to create personalized cell-based therapies that are tailored to a patient's specific needs (Mandai et al., 2017; Robinton & Daley, 2012; Shi et al., 2017). Several studies modeled complex neurologic diseases such as Parkinson and Alzheimer using iPSC derived neurons (Liao et al., 2016; Soldner et al., 2016; Yagi et al., 2011). Moreover, iPSC derived three-dimensional culture systems such as organoids are abundantly utilized due to their easy manipulation and patient-specific character (Akbari et al., 2019; Camp et al., 2015; Dye et al., 2015; Garcez et al., 2016). Large scale drug screening platforms provided by disease-specific iPSC derived cell types identified several compounds that are currently in trial to treat neurologic diseases including amyotrophic lateral sclerosis (ALS) and spinal muscular

atrophy (SMA) (Naryshkin et al., 2014; Shi et al., 2017). Excitingly, clinical trials started to test the efficacy and safety of functional cells derived from iPSCs to treat neovascular age-related macular degeneration and heart diseases (Cyranoski, 2018; Mandai et al., 2017).

1.3. Naïve and primed pluripotent stem cells

Naïve and primed pluripotent stem cells are two different states of pluripotency that refer to the developmental stage of the cells and their ability to differentiate into different types of cells. Naïve pluripotent stem cells are at an earlier stage of development and are characterized by their ability to differentiate into any cell type in the developing embryo. These cells can be derived from the inner cell mass of the pre-implantation embryo and are the most primitive and undifferentiated form of pluripotent stem cells (Ohtsuka & Dalton, 2008; Strelchenko et al., 2004; Ware et al., 2014). Primed pluripotent stem cells, on the other hand, are at a slightly later stage of development and are more restricted in their differentiation potential (Ghimire et al., 2018; Smith et al., 2009; Stadtfeld & Hochedlinger, 2010; Weinberger et al., 2016). While naïve cells can differentiate into all tissues found in an embryo, once they are "primed", they can no longer contribute to the extraembryonic tissues, acting very much like a "differentiated" cell despite maintaining a pluripotent state capable of giving rise to embryo proper. The differences between naïve and primed pluripotent stem cells have important implications for their potential use in regenerative medicine. Additionally, the ability to switch between the naïve and primed states may be important for efficiently generating specific cell types for regenerative medicine.

Mouse and human ESCs differ from each other by pluripotency states. mESCs derived from pre-implantation ICM form packed, dome shaped colonies (Ohtsuka & Dalton, 2008). On the other hand, conventional hESCs form flat and compact colonies and are dependent on TGF-β, FGF2 and IGF signaling pathways lacking the requirement of JAK-STAT activation via LIF present in mESCs (Dahéron et al., 2004; Vallier et al., 2005). In serum-free conditions, mESCs self-renew by retaining pluripotency under 2iL conditions that involves inhibition of MAPK and GSK3- β along with activation of LIF signalling (Dahéron et al., 2004; Ohtsuka et al., 2015; S. Takahashi et al., 2018). This serum-free culture condition enables the maintenance of mESCs that resemble the ICM of pre-implantation embryos. Naive mESCs are morphologically, transcriptionally and epigenetically more homogeneous and their differentiation potential to embryonic lineages is highly preserved compared to mESCs cultured in serum-containing media (Ghimire et al., 2018). In female mESCs, there are two active X chromosomes whereas female hESCs have one active, and one silenced X

chromosome (Minkovsky et al., 2012). Mouse primed pluripotent stem cells, EpiSCs, derived from post-implantation epiblasts resemble conventional hESCs with respect to previously mentioned morphology, signaling pathway dependence, and transcriptional and epigenetic programs (Stadtfeld & Hochedlinger, 2010). These observations indicate that under standard culture conditions, hESCs are primed pluripotent stem cells. Overexpression of OCT4 and KLF4 or KLF4 and KLF2 along with 2i/LIF culture conditions can result in dome-shaped hESC colonies which re-activate silenced X chromosomes, reminiscent of a naïve pluripotent state (Hanna et al., 2010). Different groups established different culture conditions involving various inhibitors, growth factors and basal media that can revert primed hESCs to naïve hESCs (Chan et al., 2013; Gafni et al., 2013; Ware et al., 2014). Therefore, it has been conclusively shown that while the conventional hPSCs culture maintains cells in a primed state, this can be reversed by applying certain culture conditions.

1.4. The role of Yamanaka factors in reprogramming

The Yamanaka factors are a set of four transcription factors, Oct4, Sox2, Klf4, and c-Myc, that have been shown to be able to reprogram adult cells into induced pluripotent stem cells (iPSCs) (K. Takahashi et al., 2007; K. Takahashi & Yamanaka, 2006). These factors work together to activate genes that are associated with pluripotency and to repress genes that are involved in the differentiation of the cell. While Oct4, Sox2, and Klf4 are responsible for activating pluripotency-related genes, c-Myc is largely involved in regulating cell growth and proliferation (Golipour et al., 2012; Hirsch, Coban Akdemir, et al., 2015; Papp & Plath, 2011; Rand et al., 2018; Z. Wei et al., 2013; Zviran et al., 2019). In addition to these factors, other transcription factors and signaling pathways can also play a role in the reprogramming process (Aarts et al., 2017; Arabacı et al., 2020; Hernandez et al., 2018; Ho et al., 2011).

Somatic cell reprogramming occurs in three stages. The first stage is called initiation and corresponds to the time interval between OSKM overexpression and mesenchymal-to-epithelial transition (MET) (Pei et al., 2019; Samavarchi-Tehrani et al., 2010; Soufi et al., 2012; Y. Wang, Chen, et al., 2020). During this stage, OSK cooperatively binds their target DNA motifs and silences the transcriptional program that maintains somatic cell identity (Chronis et al., 2017). OSK redistribute the occupancy of somatic cell-specific transcription factors (Chronis et al., 2017). This redistribution results in a decrease in the expression of somatic cell-specific genes and a concomitant increase in pluripotency-associated gene expression(Chronis et al., 2017). This silencing of the fibroblast transcriptional program

during the initial stage of reprogramming is accompanied by the mesenchymal-to-epithelial transition (MET) (Pei et al., 2019).

The duration between MET and activation of the pluripotency circuit is called the maturation stage of reprogramming. Between initial and maturation stages, reprogramming cells become more prone to cellular senescence and proliferation slows down (Aarts et al., 2017; E. J. Y. Kim et al., 2018; Rand et al., 2018; Y. Wang, Chen, et al., 2020). MYC overexpression along with OSK, provides reprogramming cells with enhanced potential to proliferate and overcome the senescence barrier (Rand et al., 2018). Endogenous pluripotency circuit must be re-activated during the maturation stage for successful pluripotency induction. OSK cooperatively bind to their regulatory element targets to activate pluripotency-associated genes (Chronis et al., 2017). In this stage, reprogramming cells start to express pluripotency markers such as alkaline phosphatase, TRA-1-60 and telomerase (Buganim et al., 2013; Firas et al., 2015; Golipour et al., 2012). Interestingly, a transient upregulation of genes related to embryonic lineages is observed which suggests that reprogramming to pluripotency traces back to development (Cacchiarelli et al., 2015; K. Takahashi et al., 2014).

The last stage of reprogramming is the maintenance stage where iPSC colonies emerge and grow in size. Exogenous transgenes are silenced and iPSCs are able to self-renew independently of OSKM transgenes(Papp & Plath, 2011). Rather than emergence of new colonies, during this stage, it is more essential for an already formed iPSC colony not to differentiate. To achieve this goal, iPSCs require activation of FGF signaling, feeder cells or a coating material such as matrigel to maintain the endogenous transcription program that keeps them in an undifferentiated state (Mossahebi-Mohammadi et al., 2020). Proper conclusion of the maintenance stage requires extensive epigenetic resetting as failure in this stage impairs self-renewal and causes spontaneous differentiation (Buganim et al., 2013).

1.5. Chromatin-based (epigenetic) barriers to reprogramming

Reprogramming of somatic cells into pluripotent stem cells is only possible through changes in epigenetic and transcriptomic state. During the initial stage of reprogramming H3K4me2 decreases at EMT genes, whereas H3K4 methylation increases at proliferation, metabolism and pluripotency genes (González & Huangfu, 2016; Koche et al., 2011). H3K27me3 levels remain the same globally but are depleted from sites where H3K4 is methylated during reprogramming. Li et al. classified ATAC-Seq signal changes during reprogramming as open to closed and closed to open, whose regulatory sites were associated with somatic and pluripotency genes, respectively (D. Li et al., 2017). This study showed that

closed to open chromatin state regulatory elements contain OSK motifs whereas open-to-closed elements do not (D. Li et al., 2017). Sin3A corepressor complex mediated activity was proposed to coordinate open-to-closed chromatin state during reprogramming by reduced H3K27ac levels at regulatory loci of somatic genes (D. Li et al., 2017). These studies pinpoint extensive chromatin remodeling induced by OSKM expression during somatic cell reprogramming to achieve pluripotency induction.

Demethylation of repressive histone marks on regulatory elements of epithelial and pluripotency related genes is necessary for iPSC generation. Ascorbic acid facilitates reprogramming via activating Jhdm1a/1b induced H3K36me2/3 demethylation which results in subsequent changes to favor pluripotency (T. Wang et al., 2011). Similarly, demethylation of H3K9me3 and H3K36me3 by KDM4B has been shown to increase reprogramming efficiency (J. Wei et al., 2017). H3K27 demethylase Utx has been shown to cooperate with OSK to activate pluripotency-circuit and its depletion resulted in inefficient reprogramming as a result of inactive H3K27me3 deposition at regulatory regions of unsuccessfully derepressed pluripotency genes (Jiang et al., 2020; Mansour et al., 2012). Another demethylase of H3K27me3, JMJD3, has been shown to positively regulate reprogramming in the same manner as previously discussed demethylases but at the same time, it impairs reprogramming by inducing Ink4a, a pro-senescence factor, expression and degrading PHF20, a pluripotency regulator (Huang et al., 2020).

Suppressing the expression of a histone chaperone, APLF, increases reprogramming efficiency and facilitates MET by upregulating CDH1, NANOG and KLF4 through depleting macroH2A from promoters and depositing H3K4me2 to the promoters of related genes (Syed et al., 2016). Depleting subunits of another histone chaperon complex CAF-1 increased reprogramming efficiency by enabling more chromatin accessibility at enhancers, increasing Sox2 binding to pluripotency genes to upregulate them (Cheloufi et al., 2015). macro-H2A was shown to occupy cis-regulatory elements of pluripotency-specific genes in somatic cells and depleted from these regions in pluripotent stem cells (Pasque et al., 2012). Removing this histone variant increases the efficiency of inducing pluripotency immensely (Pasque et al., 2012). These results showed that the interplay between histone variants and histone chaperones dictates chromatin accessibility, histone modifications, TF binding and gene expression to orchestrate pluripotency induction.

Somatic cell reprogramming to pluripotency is a well-established model to study factors that are important in safeguarding somatic cell identity as their inhibition increases reprogramming efficiency. Previous studies showed that inhibiting FACT (Kolundzic et al.,

2018), DOT1L (Onder et al., 2012; Uğurlu-Çimen et al., 2021), CBP/EP300 bromodomain (Ebrahimi et al., 2019a), BRD9 (Sevinç et al., 2022), RPAP1 (Lynch et al., 2018), SUMO (Borkent et al., 2016; Cossec et al., 2018) and BRD4 (Shao et al., 2016) facilitates reprogramming by downregulating somatic cell-specific genes. Specifically, knocking down FACT subunits, SSRP1 and SUPT16H increased human somatic cell reprogramming to both iPSC and induced neurons through downregulating somatic genes and reprogramming barriers such as PRRX1 (Ebrahimi et al., 2019a; Kolundzic et al., 2018). Importantly, the function of FACT to safeguard cell identity seems to be conserved from C. Elegans to human (Kolundzic et al., 2018). Thus, reprogramming to pluripotency serves as a useful model system to study mechanisms that help maintain cell identity.

1.6. Results of screening approaches during reprogramming

Several screening approaches have been carried out to identify barriers to reprogramming in mammalian cells. A genome-wide CRISPR-UMI screen and revealed novel human somatic cell reprogramming repressors; Pias1, an E3 SUMO-protein ligase and Men1, transcriptional cofactor (Michlits et al., 2017). Genome-wide RNAi approach identified genes related to ubiquitination (UBE2E, UBE2D and RNF40), ADAM family (ADAM7, ADAM21 and ADAM29), endocytosis (DRAM1 and SLC17A5), chromatin regulators (ATF7IP and MED19) and transcription factors (TTF2 and TMF1) as reprogramming barriers in human fibroblasts (Qin et al., 2014). The protein modifier SUMO2 is another validated top hit that blocks reprogramming from a serial genome-wide shRNA screen in mouse (Borkent et al., 2016). Another genome-wide shRNA screen revealed Tfdp1, Gtf2e1, Nfe2, Foxn3, Erf, Cdkn2aip, Msx3, Ssbp3, Dbx1, Hoxd4, Lzts1, Arx, Hoxd12, Gtf2i, Ankrd22 and Hoxc10 as novel barriers to reprogramming at its early stage in mouse (Yang et al., 2014). SMAD3 (TGF-β pathway), ZMYM2 (epigenetic modifier), SFRS11 (splicing factor), SAE1 (Sumo-activating enzyme) and ESET (H3K9 methyltransferase) are barriers to human reprogramming uncovered by a genome-wide siRNA screen (Toh et al., 2016). These genome-wide screens enabled the identification of various biological processes as barriers to reprogramming.

Various screens have focused on epigenetics rather than genome-wide approach to understand the mechanism of reprogramming through RNA regulation or chromatin modifications. shRNA screen targeting mouse USP family genes uncovered USP26 as a negative regulator of somatic cell reprogramming (Ning et al., 2017). miRNA-212/132, identified by the miRNA screen, is a barrier to reprogramming in mice (Pfaff et al., 2017). A

focused shRNA screen targeting DNA or histone methylation pathways identified H3K79 methyltransferase DOT1L, H3K9 methyltransferase SUV39H1 and context-dependent transcriptional activator or repressor YY1 (Onder et al., 2012). Another shRNA screen targeting epigenetic modifiers identified TRIM28 and SETDB1 which establish H3K9me3 to maintain somatic cell identity as novel barriers to reprogramming (Miles et al., 2017). shRNA screen targeting both known and predicted chromatin regulators revealed histone chaperone CAF-1 as a barrier to reprogramming by safeguarding somatic cell identity (Cheloufi et al., 2015). These epigenetics-focused screens have highlighted the importance of chromatin-based regulation of somatic cell reprogramming to pluripotency.

In addition to genetic screens, a number of chemical compound screens have been carried out to identify molecules that increase reprogramming efficiency. A kinase inhibitor screen identified compounds that inhibit p38, inositol trisphosphate 3-kinase and Aurora A kinase as enhancers of reprogramming efficiency (Z. Li & Rana, 2012). 5′-azacytidine (DNA methyltransferase inhibitor) and HDAC inhibitors; suberoylanilide hydroxamic acid (SAHA), trichostatin A (TSA) and VPA were found to greatly enhance mouse reprogramming efficiency through a chromatin focused compound screening using Oct4-GFP transgenic reporter (Huangfu et al., 2008). Epiblastin A was found as an enhancer of mouse EpiSC reprogramming to naïve pluripotent stem cells (Ursu et al., 2016). These inhibitor screens identified several reprogramming enhancing compounds. Additionally, two recent studies showed that chemical screens are instrumental in finding OSKM replacing compounds such as CBP/EP300 bromodomain inhibitors and LSD1 inhibitor (Ebrahimi et al., 2019a; K.-P. Kim et al., 2021). Such studies paved the way to achieve chemically induced human pluripotent stem cells (CiPSC) and further optimization of the protocol yielded much higher efficiency (Guan et al., 2022a).

Recent advances in screening novel barriers for murine cell conversions by CRISPR-Cas9 systems encouraged us to perform our own screen on human somatic cell reprogramming. To identify chromatin factors whose loss has an additive effect with DOT1L inhibition on reprogramming, a focused, pooled CRISPR-Cas9 screen in the presence of DOT1L inhibitor was performed by our group (Figure 1.1). In this screen, we targeted 247 histone modifier-coding genes' functional domains with 5 or 10 gRNAs in addition to 80 non-targeting gRNAs (Ozyerli-Goknar et al., 2022). We transduced lentiviruses containing gRNA expressing plasmids to Cas9 expressing human fibroblasts. Then, after reprogramming with OSKM factors, we sorted TRA-1-60 positive cells at the end of reprogramming (at day 21). Genomic DNA was extracted and gRNAs were amplified to add sequencing adapters at

the ends of PCR products. After deep sequencing of fragments, gRNAs were aligned to the genome to get raw count data. This was used in MaGECK algorithm to detect enriched gRNAs and target genes in TRA-1-60 positive cell population compared to day 0 of reprogramming. Along with known or currently studied chromatin factors, novel barriers such as USP22 (Ubiquitin specific peptidase 22) have been identified as a result of this screen (Figures 1.2 and 1.3).

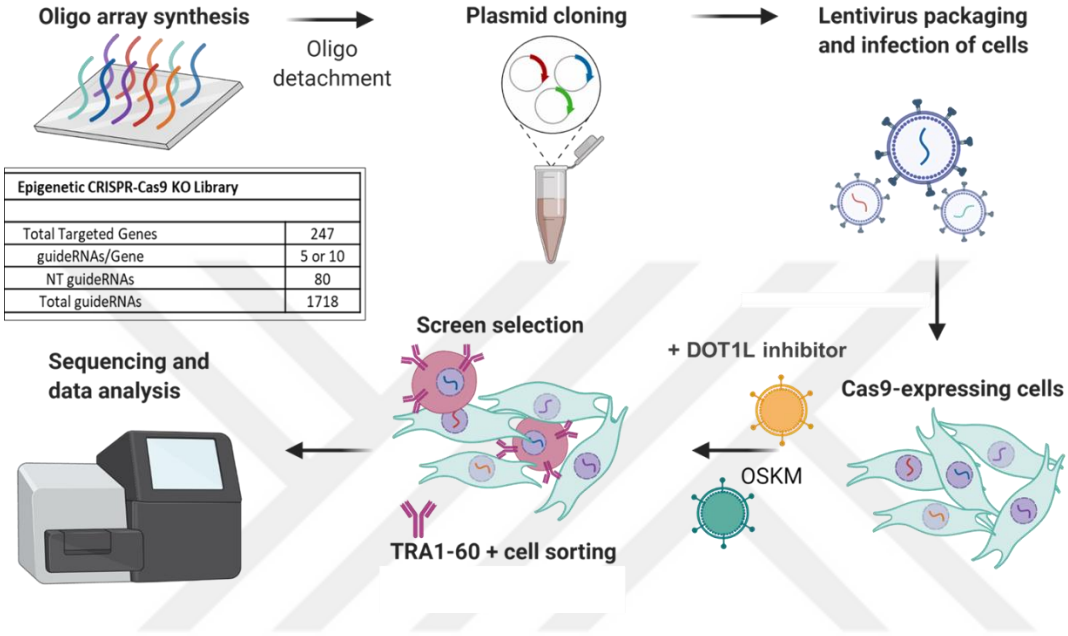

Figure 1.1. Schematic representation of the screen outline.

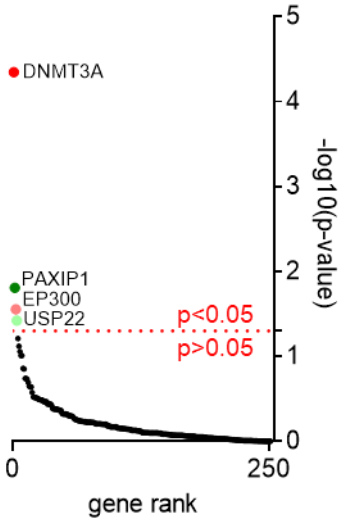

Figure 1.2. Positively selected gRNAs during reprogramming identified by MaGECK algorithm at the gene level. The red dot line indicates p-value 0.05.

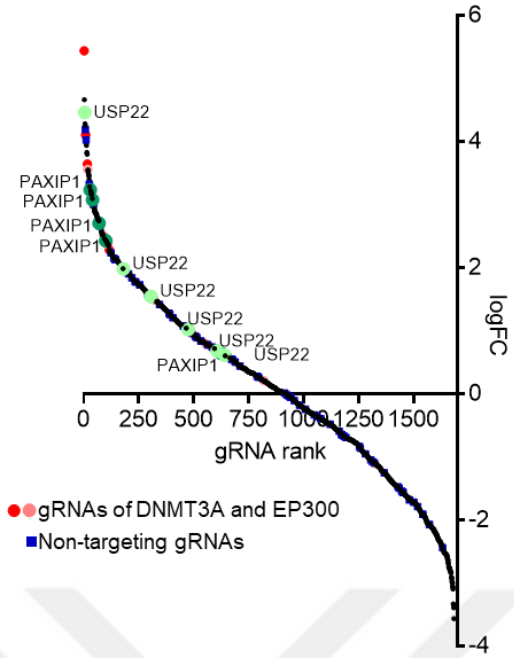

Figure 1.3. Positively selected gRNAs as a result of reprogramming, gRNAs targeting known and novel barriers and non-targeting gRNAs are highlighted.

1.7. Ubiquitin specific peptidase 22 (USP22) protein

USP22 is a member of the deubiquitinase module of SAGA (SPT-ADA-GCN5 acetylase) complex which is conserved from yeast to human (Bonnet et al., 2014). Although USP22 contains zinc-finger and deubiquitinase domains, USP22 does not have deubiquitinase activity by itself because it cannot bind to free ubiquitin (Bonnet et al., 2008; Köhler et al., 2010; Melo-Cardenas et al., 2016; Samara et al., 2010). However, USP22 requires additional regulatory proteins such as ATXN7, ATXN7L3 and ENY2 for its enzymatic activity and coupling to the remainder modules of the SAGA complex (Köhler et al., 2010; Lang et al., 2011). Additionally, there are studies that show the DUB module may function independently from the SAGA complex (Cheon et al., 2020; X. Li et al., 2017; Y. Li et al., 2017).

USP22 has both histone and non-histone protein targets. Importantly, histone ubiquitination act upstream of certain chromatin pathways that ultimately regulate the gene expression. For example, RNF20/40 ubiquitinates H2B and this is an activating post-translational modification for transcription, because it enables COMPASS and DOT1L to put active H3K4 and H3K79 methyl marks, respectively (Chandrasekharan et al., 2009; Dover et al., 2002; Henry et al., 2003; Hsu et al., 2019; Jang et al., 2019; Ma et al., 2011; Z.-W. Sun & Allis, 2002; Valencia-Sánchez et al., 2019; Worden et al., 2019, 2020). USP22 removes

this ubiquitin mark on H2B and, thus, its activity represses the transcription in that manner (Sussman et al., 2013). Conversely, PRC1 complex is a transcriptional repressor that ubiquitinates H2A which further dictates PRC2 complex to tri-methylate H3K27 (Blackledge et al., 2014; Campagne et al., 2019; Endoh et al., 2012; Pengelly et al., 2015; Tamburri et al., 2020). Again, USP22 removes this mark and, in that scenario, this deubiquitination is a derepressing activity for transcription (Lang et al., 2011). In short, USP22 has both activating and repressing roles on gene expression depending on the histone target choice. Non-histone targets of USP22 include TRF1 whose protein level is restored by USP22 leading to the maintenance of telomeric length (Atanassov et al., 2009). Additionally, USP22, deubiquitinates and stabilizes SIRT1 which leads to p53 deacetylation resulting in apoptosis suppression (Lin et al., 2012). Other USP22 target proteins include Hes1 (Kobayashi et al., 2015), SNF1 (Wilson et al., 2011), Cyclin B1 (Lin et al., 2015a), FBP1 (Nag & Dutta, 2020), RCAN1 (Melo-Cardenas et al., 2016), NFAT (Gao et al., 2014) and COX-2 (Xiao et al., 2015). USP22 removes ubiquitin modifications on these targets to stabilize them.

1.8. The role of USP22 in mammalian embryonic development

USP22 has been implicated in various cellular processes, including cell cycle regulation, DNA repair, and stem cell maintenance. In mammalian embryonic development, USP22 is essential for proper development and differentiation of various cell types. Studies in mice have shown that USP22 is required for embryonic stem cell (ESC) self-renewal and differentiation. USP22 is expressed at high levels in ESCs and is downregulated during differentiation. Knockdown of USP22 in ESCs leads to decreased self-renewal capacity and increased differentiation. In addition, USP22 has been shown to play a role in early embryonic development. Knockdown of USP22 in zebrafish embryos results in defects in embryonic development, including abnormal gastrulation and defective neural tube formation. In mice, USP22 knockout embryos exhibit defects in gastrulation and abnormal development of the nervous system. USP22 has also been shown to play a role in lineage specification during embryonic development. In mice, USP22 regulates the differentiation of neural progenitor cells into neurons and glial cells. Knockdown of USP22 in neural progenitor cells leads to decreased neuronal differentiation and increased glial differentiation. Overall, these studies highlight the importance of USP22 in mammalian embryonic development, particularly in the regulation of stem cell self-renewal and differentiation, early embryonic development, and lineage specification. These findings suggest that USP22 may be a potential therapeutic target for the treatment of several developmental disorders and

diseases associated with abnormal stem cell differentiation.

1.9. SAGA complex and interaction partners of USP22

The SAGA (Spt-Ada-Gcn5 acetyltransferase) complex is a multisubunit protein complex that is involved in the regulation of gene expression by modifying chromatin structure. The SAGA complex contains several subunits, including the histone acetyltransferase Gcn5 and the deubiquitinase USP22. SAGA complex regulates gene expression through histone modifications and transcription machinery recruitment. It consists of more than 20 proteins grouped as 5 major modules: histone acetylation module (HAT), core module, TF- (transcription factor) binding module, deubiquitination module (DUB) and splicing module (Cheon et al., 2020; Moraga & Aquea, 2015). Mutually exclusive KAT2A (GCN5) and KAT2B (PCAF) are the catalytic subunits of the HAT module of the SAGA complex (Cheon et al., 2020; Nagy & Tora, 2007; Yamauchi et al., 2000). These acetyltransferases have both histone and non-histone targets (Bonnet et al., 2014; Ghosh et al., 2018; Nagy & Tora, 2007; Yamauchi et al., 2000). TADA2, TADA3 and SGF29 are other subunits of the HAT module that coordinate to stabilize, find the substrate and target for the catalytic activity with KAT (Gamper et al., 2009; Lee et al., 2011). The core module of the complex forms the pre-initiation complex by recruiting TBP and TAF subunits that are greatly shared by TFIID generate histone octamer-like folds and TBP binding site (Baptista et al., 2017; Durand et al., 2014; Moraga & Aquea, 2015). Other proteins in this module have regulatory and structural roles for the complex (Baptista et al., 2017; Cheon et al., 2020). TF-binding module is a one large multidomain protein called TRRAP (Murr et al., 2007). This protein is a transcriptional cofactor that recruits many histone acetyltransferases including SAGA on chromatin (Liu et al., 2008; McMahon et al., 2000). Splicing module consists of SF3B3 and SF3B5 and SF3B which help to activate and properly splice some of SAGA modulated transcripts. (Cheon et al., 2020; Helmlinger & Tora, 2017; Stegeman et al., 2016; C. Sun, 2020)

USP22 is a component of the SAGA complex and interacts with several other subunits of the complex, including ATXN7L3, ATXN7, and ENY2. These interactions are important for the function of the SAGA complex in regulating gene expression. In addition, USP22 has been shown to interact with other proteins outside of the SAGA complex. One important interaction partner of USP22 is SIRT1, a histone deacetylase that plays a critical role in regulating chromatin structure and gene expression. USP22 has been shown to interact with and regulate the activity of SIRT1, which in turn affects the expression of target genes (Ao

et al., 2014; Lin et al., 2012; Ling et al., 2017). Additionally, USP22 has been shown to interact with various transcription factors and co-regulators, including p53, Myc, and E2F1 (D. Kim et al., 2017; Lin et al., 2012; Zhou et al., 2017). These interactions are thought to be important for the regulation of gene expression and cell cycle progression. Overall, the interactions of USP22 with other proteins, both within and outside of the SAGA complex, are critical for its role in regulating chromatin structure and gene expression. Understanding these interactions may provide insights into the mechanisms underlying the functions of USP22 and the SAGA complex and may have important implications for the development of therapies targeting these proteins in various diseases.

The role of various SAGA members has been investigated in the context of somatic cell reprogramming and pluripotency. Gcn5 has been found to stabilize mouse pluripotency by controlling transcriptional heterogeneity such as Nanog Moris et al., 2018). Similarly, Trrap was found to restrict mESC differentiation by promoting self-renewal (Sawan et al., 2013). Also, Gcn5 and Myc are essential factors that form an alternative splicing network during somatic cell reprogramming for an efficient reprogramming outcome (Hirsch, Akdemir, et al., 2015).

Chapter 2

MATERIALS AND METHODS

2.1. Preparation of competent cells by using rubidium chloride method

For CRISPR cloning and plasmid DNA purification, commercial Stbl-3 bacteria was streaked on an antibiotics-free agar plate and incubated at 37 °C. After 16 hours, the plate was checked and stored at 4°C. To prepare homemade competent bacteria stock, single bacteria colonies were picked and were inoculated into 2 mL antibiotic-free LB broth for overnight culture at 37°C in a bacterial orbital shaker set at 225 rpm. The next day, 0.5 ml culture was diluted into 100 ml LB broth without antibiotics and incubated for 3 hours until the OD600 value was 0.4-0.6 as determined by a plate reader. The culture was aliquoted into centrifugation tubes and incubated on ice for 15 minutes. After centrifugation at 3000 rpm at 4°C for 15 minutes, the supernatant was discarded carefully after which the pellet was washed with 16.5 ml/tube RF1 buffer (pH 5.8) which includes 100mM RbCl, 50 mM MnCl2.4H2O, 30mM potassium acetate, 10 mM CaCl2 and 15% glycerol. The suspension was placed on ice for 15 minutes before the centrifugation step was repeated. After centrifugation, tubes were again placed on ice to allow them to cool. The supernatant was removed from the conical tube then the pellet was resuspended with 4 ml/tube RF2 buffer (pH 6.8) including 10 mM MOPS, 10mMRbCl, 75mM CaCl2, 15% glycerol into ice. This resuspension was aliquoted into pre-cooled Eppendorf tubes. Aliquots were quickly transferred to liquid nitrogen and frozen. The aliquots were stored at -80°C until use.

2.2. Cloning and transformation

Enzymatic digestion of LentiCRISPR-v2 (Addgene plasmid, #52961) plasmid was performed with BsmB1 (NEB). After electrophoresis, the band was purified with MN PCR Clean up Kit. The extracted linear vector was treated with alkaline phosphatase (AP) enzyme. Specific top and bottom guide RNA sequences were taken from the GeCKO Library (Table 2.1). Each gRNA oligo (100µM) was annealed with T4 Polynucleotide Kinase (3' phosphatase minus, NEB) and T4 DNA Ligase Buffer (NEB). A total of 10 µl reaction was set at 37°C for 30 min, 95°C for 4 min and then the temperature was ramped down to 25°C at a rate of 5°C/min in a thermal cycler. Diluted (1:200) oligos were used as inserts for ligation reaction mixes which include 50 ng digested LentiCRISPR-v2 plasmid. The reactions were incubated at RT. After 2

hours, for each reaction, ligation reaction was mixed by vortexing following which 5 µl of the reaction was transferred into 50 µl competent bacteria aliquot that was thawed on ice. The mixture was incubated for at least 30 minutes on ice then heat shock was performed at 42°C for 30 seconds in a water bath. Eppendorf was replaced on ice to normalize temperature for 5 minutes before adding 150 µl SOC medium. Transformation mixture was cultured at 37°C and 225 rpm in orbital bacterial shaker. 60 minutes later, 100µl growth culture was spread on Ampicillin resistant LB agar plate. The cloning success was confirmed by U6 promoter targeted Sanger sequencing.

Table 2.1. Table of gRNAs used in cloning.

USP22_1_Top	CACCGAGTCCCGCAGAAGTGGCGTG
USP22_1 _Bottom	AAACCACGCCACTTCTGCGGGACTC
USP22_2_Top	CACCGGCAACCCGCCTGTGAAGATC
USP22_2_Bottom	AAACGATCTTCACAGGCGGGTTGCC
USP22_3_Top	CACCGGCCTCCGTACATCAGATCAA
USP22_3_Bottom	AAACTTGATCTGATGTACGGAGGCC
USP51_53394_Top	CACCGCTAGACGGGTCGGGGGATCC
USP51_53394_Bottom	AAACGGATCCCCCGACCCGTCTAGC
USP51_53395_Top	CACCGTGATCTACCAGCGTTTCGTT
USP51_53395_Bottom	AAACAACGAAACGCTGGTAGATCAC
USP51_53396_Top	CACCGGTCTTCGAGACGTGAAGCCG
USP51_53396_Bottom	AAACCGGCTTCACGTCTCGAAGACC
USP27X_53316_Top	CACCGCGCGGCGCACGACTGCGACG
USP27X_53316_Bottom	AAACCGTCGCAGTCGTGCGCCGCGC
USP27X_53317_Top	CACCGGTGAGATGTCGTCGCTGTTT
USP27X_53317_Bottom	AAACAAACAGCGACGACATCTCACC
USP27X_53318_Top	CACCGCTCGATGCCAGTTGTAGTAT
USP27X_53318_Bottom	AAACATACTACAACTGGCATCGAGC
ATXN7L3_03857_Top	CACCGGATATACGCGGACCTGGTCG
ATXN7L3_03857_Bottom	AAACCGACCAGGTCCGCGTATATCC
ATXN7L3_03858_Top	CACCGGCAGCCGAATCGCCAACCGC
ATXN7L3_03858_Bottom	AAACGCGGTTGGCGATTCGGCTGCC
ATXN7L3_03859_Top	CACCGCTCACCGGCGGTTGGCGATT
ATXN7L3_03859_Bottom	AAACAATCGCCAACCGCCGGTGAGC
ENY2_15220_Top	CACCGCAGTTGAAGGCACACTGTAA
ENY2_15220_Bottom	AAACTTACAGTGTGCCTTCAACTGC
ENY2_15221_Top	CACCGACACGTTACTGTTGATGACT
ENY2_15221_Bottom	AAACAGTCATCAACAGTAACGTGTC
ENY2_15222_Top	CACCGCTCCAGTTTCTATCAACTTT
ENY2_15222_Bottom	AAACAAAGTTGATAGAAACTGGAGC

To create USP22 g1 resistant cDNA, point silent mutation to destroy the NGG site was performed on Flag-HA-USP22 (Addgene plasmid, #22575). To achieve this Q5 site directed mutagenesis kit was utilized by following manual (NEB, cat. # E0554S). Additionally, point mutations to create K129Q, K129R and C185A were performed by primers listed on Table 2.2 by Q5 site directed mutagenesis kit. Mutations were confirmed by Sanger sequencing.

Table 2.2. List of primers used in amplifying USP22 cDNA to create indicated mutations.

Q5-22575-USP22g1-F	GTGGCGTGTGTGTCAGGGCCT
Q5-22575-USP22g1-R	TTCTGCGGGACTTCTTCCTG
Q5-22575-C185A-F	GTTCATGAAGGCTGTGTTCCCAAGGTTGATCAGCC
Q5-22575-C185A-R	TGCATCGTGCAGGCCCTG
Q5-22575-K129Q-F	TGCTCCTCCTGGGCGATTATT
Q5-22575-K129Q-R	GCGAAAAGCTTGGAAAATG
Q5-22575-K129R-F	CTGCTCCTCCCTGGCGATTAT
Q5-22575-K129R-R	CGAAAAGCTTGGAAAATGCAAG

2.3. Plasmid DNA isolation

Single bacterial colonies were picked into 100-200 ml LB-Broth with the specific antibiotic from the LB agar plate. Suspension cultures were grown at 37°C and 225 rpm in a bacterial orbital shaker. After O/N incubation, bacterial cultures were transferred to the conical tubes and centrifuged at 4°C and 3750 rpm for 30 minutes. Supernatants were removed and pellets were kept at -20°C until plasmids were purified by Macherey-Nagel (MN) midi-prep kit. If a plasmid DNA was isolated from commercial stab plasmid culture (Addgene), the culture was started by streaking the bacteria to generate single colonies. The other steps were followed as mentioned above.

2.4. Supernatant and concentrated virus production

$2x10^6$ HEK 293T cells were seeded into 10-12 ml complete DMEM medium including 10% FBS, 1% Pen-Strep in high glucose DMEM 1X, on 10 cm culture dishes. On the following day, cells were transfected with mixture of the viral packaging plasmids (250 ng the envelope protein encoding plasmid (VSV-G), 2250 ng Gag-Pol (pUMVC for retroviruses and psPAX2 for lentiviruses) and 2500 ng viral plasmid DNA by FuGENE® 6 Transfection Reagent (Promega). The DNA and reagent tubes prepared separately were made up to 200 µl each with serum-free DMEM. These tubes were mixed before 30 minutes of incubation at RT. Then, transfection reagent and DNA mixtures were added onto HEK293T medium. 16 hours later, the medium was refreshed. Supernatants were collected into conical tubes at 48 and 72 hours. To remove

HEK293T cells from the supernatant, tubes were centrifuged and filtered through a 0.45µm sterile syringe filter then aliquoted in Eppendorf tubes and stored at -80°C until use. To prepare a concentrated virus, 50% PEG8000 was added into the filtered supernatant at 1:4 ratio and mixed. After 48 hours, tubes were centrifuged at +4°C. Pellet was resuspended with DPBS at a concentration of 100x and aliquoted.

2.5. iPSC and fibroblast viral infection and marker specific selection

To generate knock-out single cell clones iPSCs, cells were expanded up to 80% confluency then split 1:10 ratio in 6 well plates with the ROCK inhibitor, Y-27632 in mTeSR Plus medium (Stem Cell Technologies, cat # 100-0276). Next day, the medium was changed with fresh and ROCK inhibitor-free medium. A few days later, concentrated viruses were mixed with 1 ml medium containing protamine sulfate (8 µg/ml). Then the medium was changed. After 16 hours incubation, viruses including medium was changed with 2 ml fresh medium. The puromycin selection was performed after 2 days. At the end of selection, cells were split and expanded to check the knockout phenotype by western blot. Serial dilution was performed to seed single cells into 96 well plates. Single clones were expanded and western blot was performed to verify if they were knockout clones.

Fibroblast cells were counted and seeded at specific ratio ($1x10^5$ cells/ well into 6 well plates). Cells were infected with 1 ml viruses, 200µl fresh medium and protamine sulfate (8 µg/ml) after 24 hours from seeding. Next day, the infection was repeated (optional). After infections, cells were split at 1:3 following which puromycin selection was performed (1 µg/ml).

2.6. Preparation of inactivated mouse embryonic fibroblast for stem cell culture

At day E13, pregnant Balb/c mice were sacrificed by cervical dislocation. Embryos were separated from the surrounding membranes, placenta, brain and other red organs. Blood was removed by washing with PBS. Embryos were minced finely with a razor blade until they became pippettable. Each embryo was resuspended in 2 mL of 0.05% trypsin-EDTA and incubated at 37°C for 15 minutes. For each embryo, 4 mL D10 (10% FBS, 1% Pen-Step in DMEM) media was added to inactivate trypsin before removing any remaining large pieces. After centrifugation at 1500 rpm for 5 minutes, the pellet was resuspended in 5 mL D10 (10% FBS, 1% Pen-Strep in DMEM) media per embryo. Two embryos were plated at passage 0 in a precoated (0.1% gelatin) 10 cm dish. After MEFs reached confluency, they were detached in 2 ml of 0.05% trypsin-EDTA per each dish at 37°C for 5 minutes. 4 mL D10 (10% FBS, 1% Pen-Strep in DMEM) per each dish was used to deactivate trypsin and cells were centrifuged at 1500 rpm for 5 minutes. Pellet was resuspended in 1 mL freezing media (90% FBS, 10%

DMSO) per each dish. They were aliquoted in cryovials and stored at -80 °C.

Confluent MEFs in 15 cm dishes at passages 4 or 5 were washed once with PBS to inactivate them mitotically. 10 mL D10 (10% FBS, 1% Pen-Strep in DMEM) containing 10 µg/mL mitomycin C was added to each plate and cells were incubated at 37°C for 2 hours. The plates were washed twice with PBS and 5 mL 0.05% trypsin-EDTA per each dish was added. After 5 minutes incubation at 37°C, trypsin was inactivated with 10 mL D10 media (10% FBS, 1% P en-Strep in DMEM). Cells were counted with a hematocytometer and resuspended in freezing media (90% FBS, 10% DMSO) to correspond to a specific number of cells at each cryovial.

dH1f cells were differentiated from H1 ESCs for a month using D10 media (10% FBS, 1% P en-Strep in DMEM). At passages 13-15, dH1f cells were seeded at a density of 50**,**000 cells per well of a 12-well plate and transduced overnight with pSIN4-EF2-O2S (Addgene, plasmid, #21162) and pSIN4-CMV-K2M viruses (Addgene, plasmid #21164). On day 6 after OSKM overexpression, dH1f cells were passaged onto 0.1% gelatin pre-coated, mitomycin-C-treated MEF seeded, 12-well plates at a one eighth ratio. The next day, the medium was changed to hES medium (20% Knock Out Serum Replacement (Gibco, cat. # 10828028), 1% NEAA, 1% Pen-Strep, 1% L-glutamine, 55µM 2-Mercaptoethanol, 10 ng/mL b-FGF in DMEM/F12). Cells were fixed with 4% paraformaldehyde between 18 and 21 days of reprogramming and TRA-1-60 staining was performed to quantify reprogramming efficiency.

2.7. Episomal nucleofection

This assay was performed before as described using adult skin fibroblast cells (Sevinç et al., 2022).

2.8. Cell surface marker TRA-1-60 PE staining and flow cytometer

This experiment was performed as described earlier (Sevinç et al., 2022).

2.9. TRA-1-60 HRP DAB staining, quantification, and ImageJ analysis

Human iPSC colonies were quantified via TRA-1-60 immunostaining. Paraformaldehyde-fixed cells were washed once with PBS and incubated with biotin-anti-TRA-1-60 (eBioscience, cat. # 13-8863-82) or at 1:200 dilution in staining solution (3% FBS, 0.3% TritonX-100 in PBS) overnight at 4°C. Next day, cells were washed twice with PBS and incubated with streptavidin horseradish peroxidase (Biolegend, cat. # 405210) at 1:500 dilution in the staining solution for 2 hours at room temperature. A master mix of DAB solution was prepared by adding and vortexing in DAB solution (0.1% 3,3'-diaminobenzidine (Sigma D8001), 0.05% nickel ammonium sulfate and 0.015% H_2O_2 in PBS). Brown color development should be present

after 10 minutes of incubation at room temperature. Cells were washed twice with PBS. Cream was used to cover the surface of wells to create contrast during the scanning of the plates. Plates were scanned in JPEG format by at least 600 dpi resolution and analyzed by ImageJ software (https://imagej.nih.gov/ij/).

2.10. Cell proliferation assay

This assay was performed as described earlier (Sevinç et al., 2022).

2.11. Embryoid body formation assay

Individual iPSC colonies reached 80% confluency and were detached from wells and incubated at 37°C for 5 minutes. Single cells were seeded at 96-well U bottom ultra-low attachment plates in EB medium. After 1-2 days, cells were transferred to 6-well plates and incubated on a shaker (110 rpm) at 37°C for up to 6 days.

2.12. Teratoma assay

This assay was performed as described earlier (Sevinç et al., 2022).

2.13. Protein extraction

Cell pellets were dissolved in lysis buffer (50 mM Tris, pH 7.4, 250 mM NaCl, 5 mM EDTA, 50 mM NaF, 1% Noidet P40, 1 mM PMSF, 1X protease inhibitor and 0.025% NaN_3). Resuspended cells were incubated on ice for 30 minutes with 10 minute vortexing intervals. They were centrifuged at 13,000 rpm for 10 minutes at 4^{o}C on a tabletop centrifuge. Supernatant containing whole cell lysate was transferred to a new tube. Protein concentrations were quantified using the Pierce™ BCA Protein Assay Kit (Thermo Fisher Scientific, cat. # 23225) 50 µg of each lysate was incubated at 95°C for 15 minutes with 4X Laemmli buffer (Bio-Rad) containing β-mercaptoethanol (Bio-Rad).

2.14. Western blotting

Boiled samples and protein marker (Bio-Rad, cat. # 161-0374) were loaded onto pre-cast SDS-PAGE gels (Bio-Rad, cat. # 456-1084). Using Bio-Rad trans-blot turbo transfer system at mixed weight transfer settings, proteins were transferred onto PVDF membrane (Bio-Rad, cat. # 1620177), followed by incubation in 5% blotting grade blocker (Bio-Rad, cat. # 1706404) solution for 1 hour. Membranes were incubated with antibodies against USP22 (NOVUS, cat. # NBP1-49644), Ubiquityl-Histone H2A (Lys119) (Cell Signaling, cat. # 8240S), Ubiquityl-Histone H2B (Lys120) (Cell Signaling, cat. # 5546S), H2B (Abcam, cat. #ab52599-1:20000),

Tubulin and GAPDH (Abcam, cat. #ab9485) at 1:1000 ratio overnight at 4°C. Next day, membranes were washed with TBS-T for 15 minutes three times and incubated with secondary antibodies (Abcam, cat. # ab97051 or ab97023) at 1:5000 ratio in blocking solution for 1 hour at room temperature. Membranes were washed with TBS-T for 15 minutes 3 times and incubated shortly with ECL western blotting substrate (Thermo Fisher Scientific, cat. #32209) before imaging using an Odyssey Imaging System (LICOR Biosciences).

2.15. Immunofluorescent staining and imaging

iPSCs were split onto coverslips with inactivated MEFs in hESC medium for immunofluorescence-based characterization as described earlier using OCT4 (Abcam, cat. # ab19857) and NANOG (Abcam, catalog no. ab21624) antibodies.

2.16. Genomic DNA isolation and PCR

To extract genomic DNA from cells, tissue isolation kit (Nucleospin, cat. # 740952.50) was used following manufacturer's instructions. DreamTaq DNA polymerase (Thermo Fisher Scientific, cat. # K1081) was used to amplify 200 ng genomic DNA with primer pairs (Table 2.3) using a Bio-Rad T100 thermal cycler with 30 cycles of 30 s at 95 °C, 30 s at 67 °C and 60 s at 72 °C.

Table 2.3. List of primers used to amplify target gDNA.

ENY2-F	ACCCAGATGAAATGAAAGGCC
ENY2-R	GGCTCCCCTTAGTGACATGTATA
ATXN7L3-F	AATTGGGGCAAACACACTCC
ATXN7L3-R	TACGTCGCTGTATCTGGCAT

2.17. T7 endonuclease assay

This experiment was performed using PCR products containing ATXN7L3 and ENY2 indel as previously described (Sevinç et al., 2022).

Human naïve reprogramming

Fibroblast cells were detached with trypsin (0.05%) and counted. Cells were seeded into 12 well plate as to be $5x10^4$ cells/ well. Next day, cells were infected with OSKM viruses (total volume was 700µl). On day 6, cells were transferred onto cell cycle arrested MEF at 1:4 ratio and switched culture medium to a HENSM-ACT medium (naïve maintenance medium). Dome-shaped naïve iPSC colonies were observed at day 9 or 10 and finalized reprogramming process at day 14. Colonies were fixed with 4% PFA solution. IF staining was performed with KLF17 (Atlas Antibodies, cat # HPA024629) or TRA1-60 antibodies (Biolegend, cat # 330604). If

limited colonies were generated, stained colonies would be counted with the naked eye otherwise Image J software was used.

2.18. Primed to naïve conversion

Primed iPSCs were seeded on Geltrex (Thermo Fisher Scientific, cat. # A1413302) coated wells in 12 well plate at 1:10 ratio in E8 media. After 2 days, cells were treated with HENSM. At the end of conversion, cells were split once every 4 days using PBS-EDTA.

2.19. TSC induction and maintenance

Naïve iPSCs were seeded on Geltrex coated wells at 1:10 ratio into TSC induction medium (TI medium: DMEM/F12, 1% N2, 2% B27, 1% NEAA, 1% Pen/Strep, 1% Sodium pyruvate, 50 ug/ml L-ascorbic acid 2-phosphate, 1% Glutamax, 0.5 µM A83-01) to start the induction process. Medium was changed every 2 days. On day 6, pellets were collected to check TSC (TP63, GATA2, GATA3) and pluripotency specific (SOX2, POU5F1) mRNA expression levels. At the same time, cells were transferred onto Collagen type IV coated plate for maintenance. Cells were split when they were 80% confluent. After 4 passages, homogeneous cell populations were present. The TSC identity was also confirmed by GATA3 (Invitrogen, cat # MA1-028) IF staining (Viukov et al.,2022).

2.20. RNA isolation and cDNA conversion

NucleoSpin RNA kit (Macherey Nagel) was used to extract total RNA from cells using manufacturer's instructions. 1 µg total RNAs from each sample were mixed with 2.5 µL of 2.5 mM dNTPs, 1 µL of 50 µM random hexamers up to a total volume of 16.5 µL in a PCR tube. This reaction was incubated at 65 °C for 5 minutes in a thermocycler and placed on ice for a while. 5 µL of 5X First Strand Buffer, 2 µL of 0.1 M DTT and 0.5 µL Rnasin (Promega, cat # N2111) was added into each tube and mixed. Reaction was incubated for 10 minutes at room temperature and 1 µL of MMLV RT (Invitrogen, cat # 28025-013) enzyme was added to each tube and mixed. Reaction was incubated at 37 °C for 1 hour and 70 °C for 15 minutes in a thermocycler. 75 µL of nuclease free water was added to each tube.

2.21. RT-qPCR

This assay was performed as described earlier (Sevinç et al., 2022). RT-qPCR primers are listed in Table 2.4.

Table 2.4. List of RT-qPCR primers used.

GATA2-F	ACTACAGCAGCGGACTCTTCCACC
GATA2-R	CAGTTGACACACTCCCGGCCTT
GATA3-F	CTACTACGGAAACTCGGTCAGGGC
GATA3-R	AGCCAGGGTAGGGATCCATGAAG
TP63-F	TTCGACGTGTCCTTCCAGCAGTC
TP63-R	GGCATGTCTTTGCAATTTGGCAG
SOX1-F	GGGAAAACGGGCAAAATAAT
SOX1-R	TTTTGCGTTCACATCGGTTA
PAX6-F	TGTCCAACGGATGTGTGAGT
PAX6-R	TTTCCCAAGCAAAGATGGAC
DPPA3-F	CGCATGAAAGAAGACCAACAAACAA
DPPA3-R	TTAGACACGCAGAAACTGCAGGGA
DNMT3L-F	CAGTGCCTGCTCCTTATGGCT
DNMT3L-R	TGAACAAGGAAGACCTGGACG
KLF17-F	AGCAAGAGATGACGATTTTC
KLF17-R	GTGGGACATTATTGGGATTC
DPPA5-F	TGCTGAAAGCCATTTTCG
DPPA5-R	GAGCTTGTACAAATAGGAGC
POU5F1-F	CCTCACTTCACTGCACTGTA
POU5F1-R	CAGGTTTTCTTTCCCTAGCT
SOX2-F	TCAGGAGTTGTCAAGGCAGA
SOX2-R	GGGCTCAAACTTCTCTCCCT
EOMES-F	GTGCCCACGTCTACCTGTG
EOMES-R	TGGTGGCGGTGGAATTTGAG
TBXT-F	ACGCAGTTCATAGCGGTGAC
TBXT-R	CAATTGTCATGGGATTGCAG
SOX17-F	GTGGACCGCACGGAATTT
SOX17-R	GGAGATTCACACCGGAGTCA
GATA6-F	GTGCCCAGACCACTTGCTAT
GATA6-R	TGGAATTATTGCTATTACCAGAGC

2.22. Gene expression analysis and RNA sequencing

Human fibroblasts were transduced by Cas9 and USP22 sg1 or sgNT1 gRNAs. Puromycin selection was performed to select cells. At day 14 of transduction, cells were transduced by OSKM vectors to reprogram them. At the day 6 of reprogramming, total RNA was extracted from cells using Direct-zol kit (Zymo Research) by following manufacturer's instructions in duplicates per sample. Libraries were prepared using Truseq stranded mRNA kit to create a first stranded library. 20-25 million paired-reads were targeted per each replicate of a sample by sequencing libraries in Novaseq 2x100bp Reads were quantified by Salmon and STAR for each transcript. The DESeq2 package was used to find differentially expressed genes between

samples. Genes were considered to be differentially regulated based on adj-$p < 0.05$. Rank-ordered gene lists were used for gene-set enrichment analysis (Subramanian et al., 2005).

2.23. Statistical Analysis

GraphPad Prism-8 was used for statistical analysis (t-tests). The details about replicates of samples are mentioned in the figure legends.

2.25. Data Availability

RNA sequencing data was registered in the NCBI GEO database with accession number GSE225151.

Chapter 3

RESULTS

3.1.The effect of CRISPR-Cas9 mediated USP22 knock-out on reprogramming

To validate the results of the CRISPR-Cas9-mediated knockout screen (Figure 1.2), individual gRNAs were cloned into the LentiCRISPR-v2 backbone. These gRNAs target novel hits identified by the screen; PAXIP1 and USP22. Human fibroblasts were infected with gRNA and Cas9 expressing plasmids and 2 weeks later they were reprogrammed to iPSC by OSKM expression. At the end of reprogramming, TRA-1-60 positive colonies were quantified to assess reprogramming efficiency. These results showed that targeting PAXIP1 did not affect the reprogramming efficiency whereas USP22 knockout significantly increased the efficiency 2- to 3-fold (Figure 3.1). This result indicated that PAXIP1 was a false positive hit of the screen, but validated USP22 as a potential barrier to reprogramming.

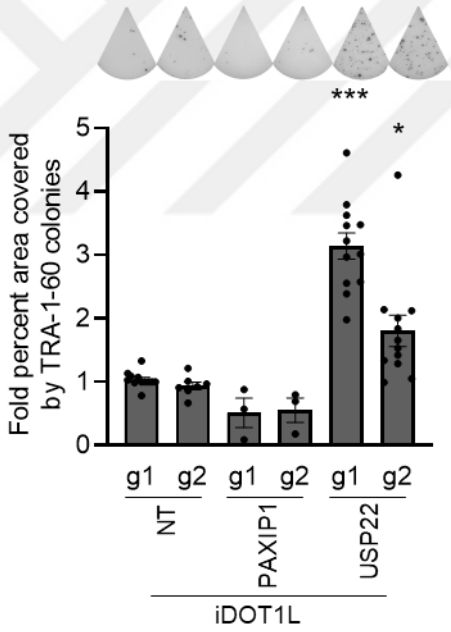

Figure 3.1. Fold change in reprogramming efficiency upon hit targeting gRNA expression. Error bars indicate the error of mean. n=3, independent experiments were conducted for PAXIP1 gRNA expression and n=12, independent experiments for USP22 gRNA expression. * Stands for $p<0.05$, ** for $p<0.005$ and *** for $p<0.0005$.

The screen and screen validations were performed in the background of DOT1L inhibition background and it was important to show if USP22 knockout alone could increase reprogramming efficiency. To achieve this goal, USP22 was targeted by three different gRNAs.

Western blot of the whole cell lysates showed that each of these gRNAs successfully depleted USP22 at the protein level (Figure 3.2). When these cells were reprogrammed to iPSCs, reprogramming efficiency increased up to 3-fold compared to the NT1 gRNA expressing cells.

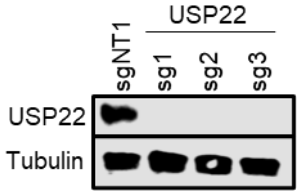

Figure 3.2. Western blot image showing USP22 protein level of USP22 targeting gRNAs in fibroblasts. Tubulin was used as a loading control.

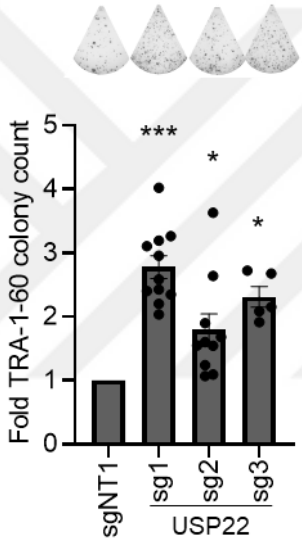

Figure 3.3. Fold change in reprogramming efficiency upon USP22 targeting gRNA expression. Error bars indicate the error of mean. n=11, independent experiments were conducted for USP22 sg1 expression, n=10 for USP22 sg2 expression and n=5 for USP22 sg3 expression. * Stands for $p<0.05$, ** for $p<0.005$ and *** for $p<0.0005$.

In order to eliminate the possibility that reprogramming phenotype of USP22 knockout is particular to lentivirus-mediated reprogramming of a specific cell line, I knocked out USP22 in a different human adult fibroblast cell line (Figure 3.4). When OSKM factors were provided by episomal vectors, instead of lentiviral vectors, the reprogramming efficiency again increased around 3-fold upon USP22 knockout which was further enhanced with additional DOT1L inhibition (Figure 3.5). These results showed that USP22 knockout increases reprogramming efficiency independent from the OSKM delivery method and fibroblast line.

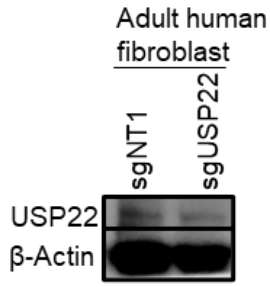

Figure 3.4. Western blot image showing USP22 protein level of USP22 targeting gRNA in human adult fibroblasts. Actin was used as a loading control.

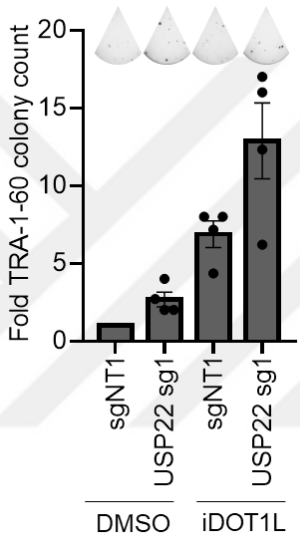

Figure 3.5. Fold change in episomal vector-induced reprogramming efficiency upon USP22 targeting gRNA expression in human adult fibroblasts. Error bars indicate the error of mean. n=4, independent experiments. * Stands for $p<0.05$.

3.2.Rescue of USP22 knock-out reprogramming phenotype by overexpression of wild-type and catalytic-mutant USP22

To further investigate the effect of USP22 on reprogramming, we attempted to rescue the USP22 loss phenotype by overexpressing wild-type and several mutant USP22s (Figure 3.6). USP22 K129 acetylation is important for its recruitment to the SAGA complex (Armour et al., 2013). To mimic USP22 acetylation, we generated a K129Q mutation based on a previous report (Armour et al., 2013). Additionally, a K129R mutant USP22 was generated to determine the effects of loss of acetylation. Lastly, we utilized the C185A mutant USP22 which has been shown to completely lack catalytic activity (Lin et al., 2015b; Roedig et al., 2021; Y. Wang,

Sun, et al., 2020).

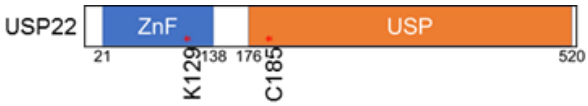

Figure 3.6. Diagram showing USP22 protein's domains and amino acid positions that are mutated.

To check the expression levels of these mutants in NT1 and USP22 sgRNA expressing cells, I performed western blot of whole cell lysates. Western blot showed that USP22 gRNA expressing cells lacked USP22, whereas various re-introduction of PAM-mutant wild-type and mutant USP22 cDNAs could be overexpressed (Figure 3.7). C185A and K129R mutations were expressed at lower levels compared to the wild-type and K129Q mutant USP22.

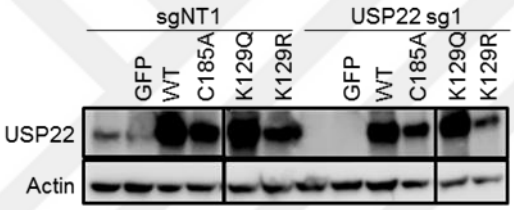

Figure 3.7. Western blot image showing USP22 protein levels after USP22 overexpression in both non-targeting and USP22 targeting gRNA expressing fibroblasts. Actin was used as a loading control.

To compare global changes in H2B ubiquitination levels upon USP22 overexpression, I performed western blot of histones extracted from nuclei. Results showed that USP22 gRNA expression did not change the global H2Bub levels, whereas C185A catalytic mutation increased the global histone ubiquitin levels (Figure 3.8). This suggests that although USP22 has been associated with histone deubiquitination, its loss may be compensated by other USP family members such as USP27X and USP51.

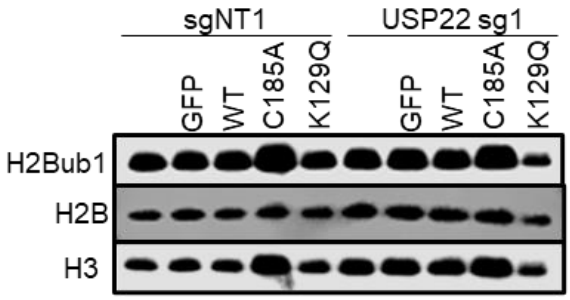

Figure 3.8. Western blot image showing H2Bub protein levels after USP22 overexpression in both non-targeting and USP22 targeting gRNA expressing fibroblasts. H3 and H2B were used as loading controls.

When USP22 cDNA expressing cells were reprogrammed to iPSCs, we observed that USP22 expression in NT1 expressing cells did not change the reprogramming efficiency (Figure 3.9). As expected, USP22 loss increased the efficiency approximately 3-fold, whereas re-expression of the various USP22 mutant cDNAs all rescued the reprogramming phenotype. These results suggest that USP22's catalytic function and incorporation into the SAGA complex do not act as barriers to reprogramming. In other words, USP22 can impede reprogramming independent of its catalytic function.

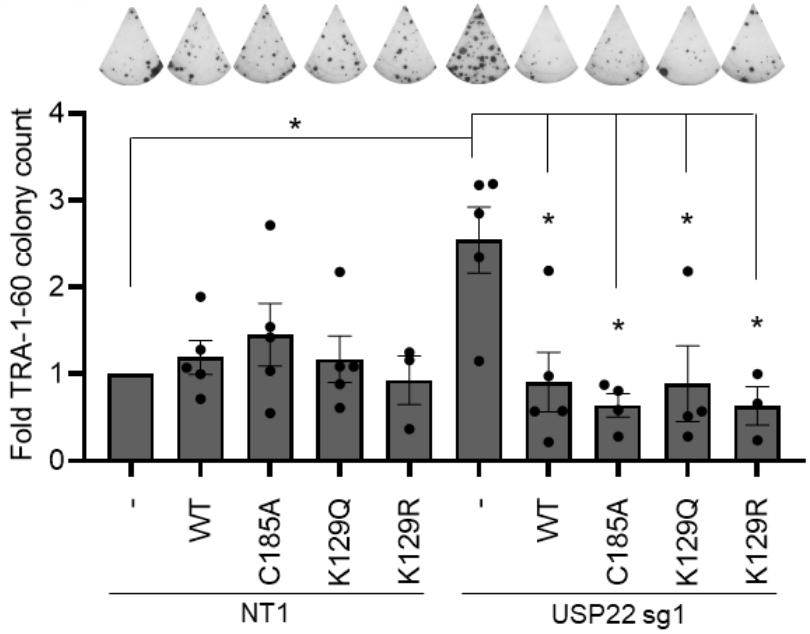

Figure 3.9. Fold change in reprogramming efficiency upon USP22 overexpression in both wild-type and USP22 knockout background. Error bars indicate the error of mean. n=3, independent experiments for KR mutations, n=4 for CA and KQ mutations in USP22 knockout background and n=5 for other comparisons. * Stand for $p<0.05$.

3.3.Determining whether the USP22 reprogramming phenotype is dependent on the SAGA complex

To determine if USP22's interaction partners in the SAGA DUB module has any effect on reprogramming, we knocked out ATXN7L3 and ENY2 with 2 independent gRNAs (Figure 3.10). Western blot of the histone extraction showed that both ATXN7L3 and ENY2 knockouts increased global histone ubiquitin levels (Figure 3.11). Additionally, by T7 endonuclease assay, we showed indel formations by each gRNA on *ATXN7L3* and *ENY2* genes (Figure 3.12). ATXN7L3 and ENY2 interact with USP27X or USP51 both of which compete with USP22 (Figure 3.13). Interestingly, ATXN7L3, USP27X and USP51 knockouts did not increase the reprogramming efficiency whereas ENY2 knockout was detrimental to iPSC generation (Figure 3.14). These results showed that neither USP22 competitors nor DUB module interactors are barriers to reprogramming.

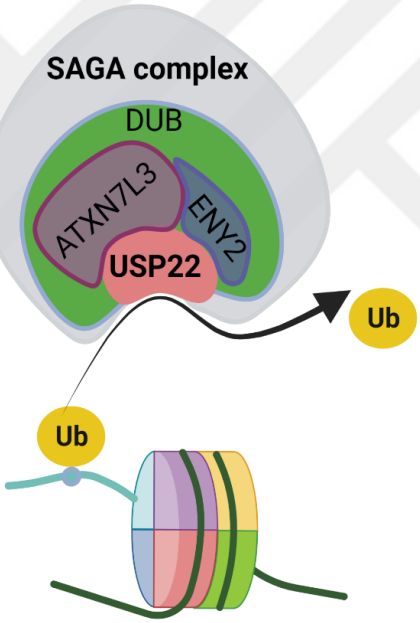

Figure 3.10. Schematic representation of SAGA complex DUB module members and deubiquitinase function.

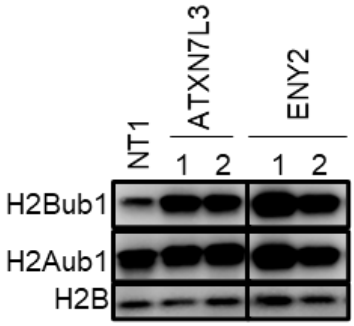

Figure 3.11. Western blot image showing H2Bub and H2Aub protein levels after ATXN7L3 or ENY2 knockouts in fibroblasts. H2B was used as a loading control.

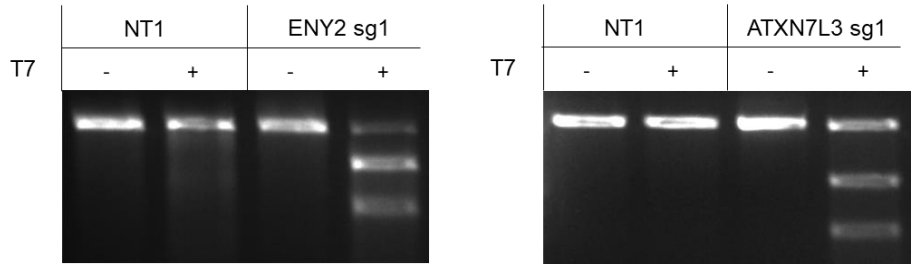

Figure 3.12. T7 endonuclease assay showing Cas9 mediated in-del formation from genomic DNA PCR products of indicated cells.

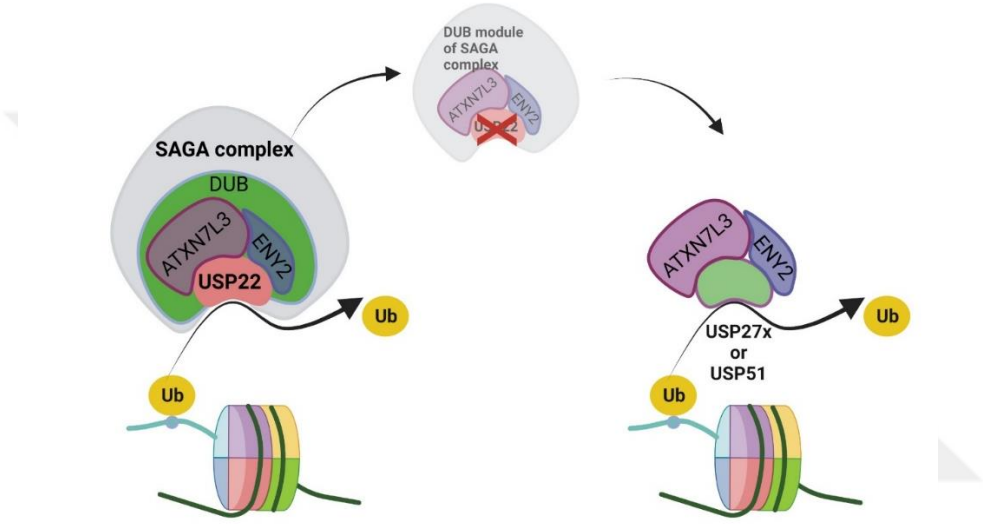

Figure 3.13. Schematic representation of SAGA independent DUB variants

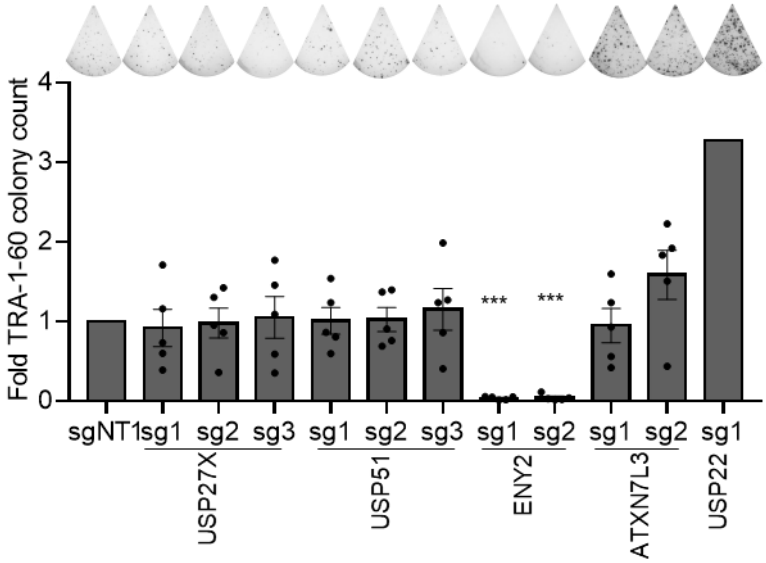

Figure 3.14. Fold change in reprogramming efficiency upon ATXN7L3, ENY2, USP27X or USP51 knockouts. Error bars indicate the error of mean. n=5, independent experiments. *

Stands for p<0.05, ** for p<0.005 and *** for p<0.0005.

3.4.USP22 stabilizes maturation stage of reprogramming for faithful pluripotency acquisition

In order to determine if USP22 loss increases reprogramming efficiency due to enhanced cell proliferation, we measured cell proliferation rate using a luminescence/ATP-based assay on uninduced and OSKM-induced cells for 6 days. Results showed no significant proliferation change during the initial stage of reprogramming or in uninduced cells (Figure 3.15). This suggests that USP22 loss does not increase reprogramming efficiency due to enhanced proliferation rates.

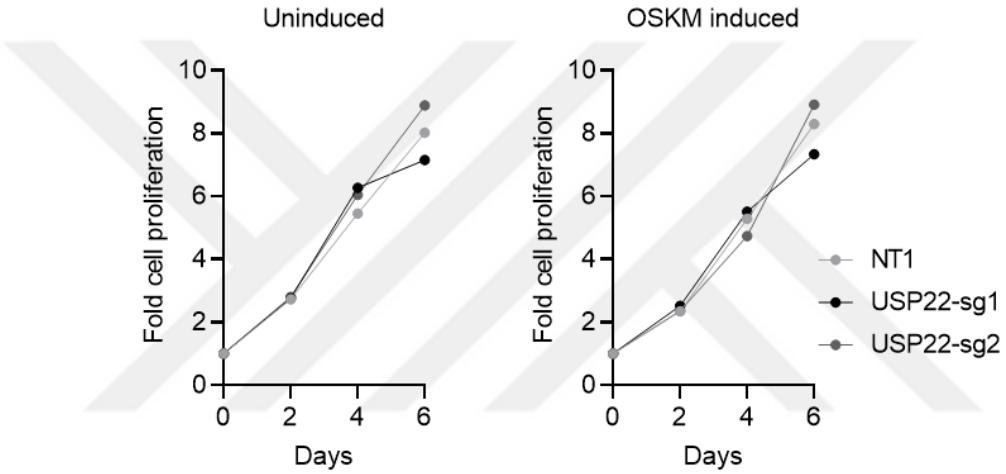

Figure 3.15. Fold change in the cell number at indicated days for uninduced (left) and OSKM induced (right) fibroblasts. One of two independent experiments was plotted.

To determine if the initial stage of reprogramming is sensitive to USP22 loss, we performed flow cytometry to detect TRA-1-60 positive cells on day 6 of reprogramming. We found that USP22 loss did not change the percentage of TRA-1-60 positive cells at this early time-point (Figure 3.16). This result indicates that USP22 does not block the emergence of early reprogrammed cells but may rather act as a barrier to later stages of reprogramming such as the subsequent maturation stage.

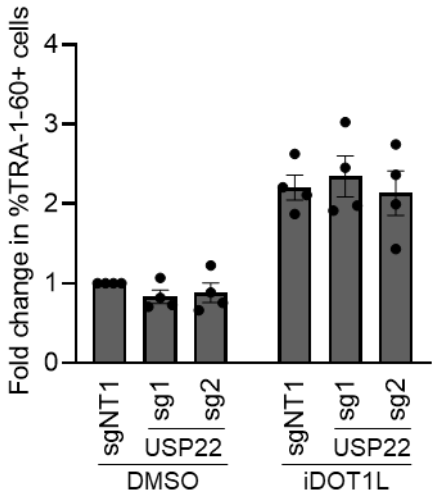

Figure 3.16. Fold change in the number of TRA-1-60 positive cells at day6 of reprogramming. Error bars indicate error of mean and n=4, independent experiments.

3.5.Determining the genes regulated by USP22 loss

To detect the genes regulated by USP22 loss during reprogramming, we performed total mRNA-sequencing (RNA-seq). RNA samples were collected from control and USP22 knockout fibroblasts 6 days after OSKM expression. To validate if the analysis and experiments were conducted correctly, distance matrix and principal components of analysis were performed (Figure 3.17 and 3.18). These results showed that biological replicates of the same experimental groups were closer to each other than those of different conditions. MA-plot and number of differentially regulated genes showed that the number of downregulated genes is higher than upregulated genes upon USP22 loss (Figure 3.19 and 3.20).

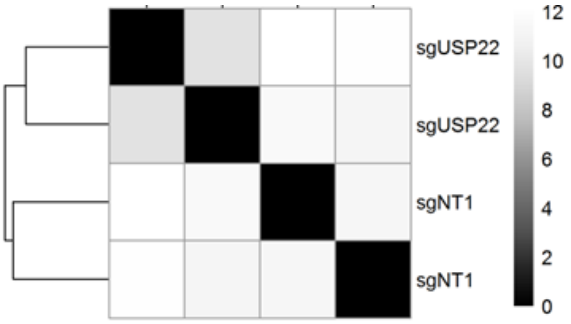

Figure 3.17. Distance matrix of transcriptome for indicated cells.

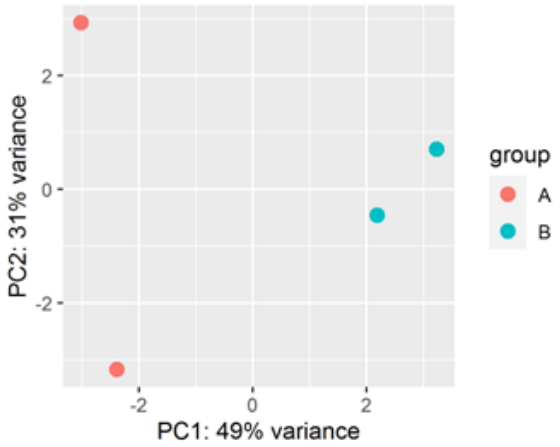

Figure 3.18. PCA of RNA-Seq samples. Group A represents NT1 gRNA expressing cells and group B represents USP22 gRNA expressing cells in biological duplicates.

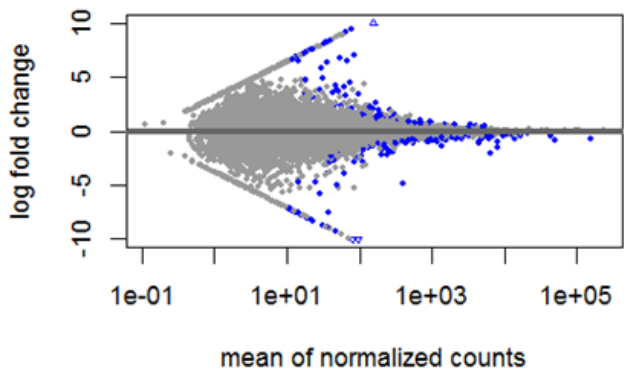

Figure 3.19. MA-plot for USP22 knockout and NT1 comparison.

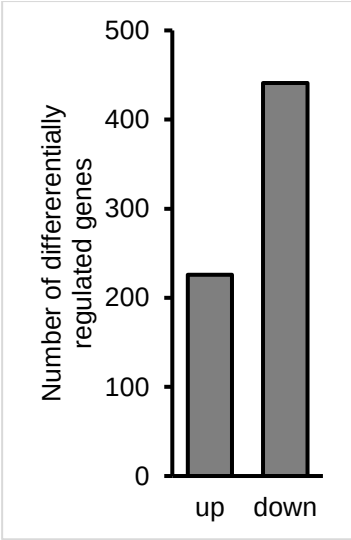

Figure 3.20. Number of differentially expressed genes upon USP22 loss during reprogramming.

3.6.USP22 loss stabilizes pluripotency network during reprogramming

In order to investigate the genes regulated by USP22 loss, we performed gene-ontology enrichment for upregulated and downregulated genes. In addition to cell cycle related genesets, pluripotency-related genesets such as SOX2, SALL4, MYC and NANOG target gene sets were enriched in upregulated genes upon USP22 loss (Figure 3.21-A). Downregulated genes were enriched among development-related genesets (Figure 3.21-B).

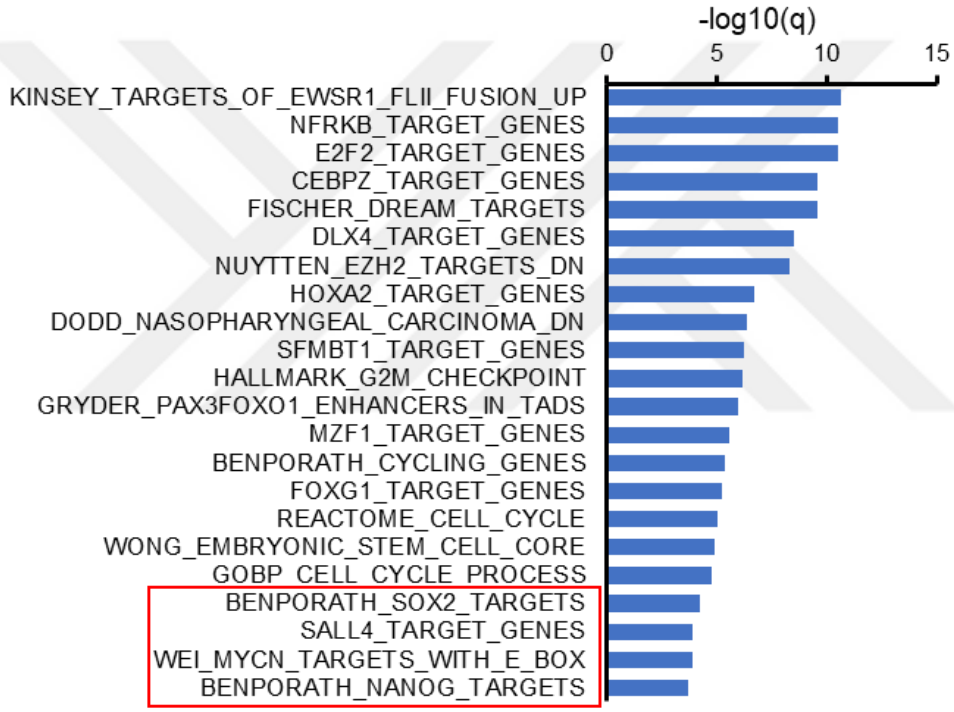

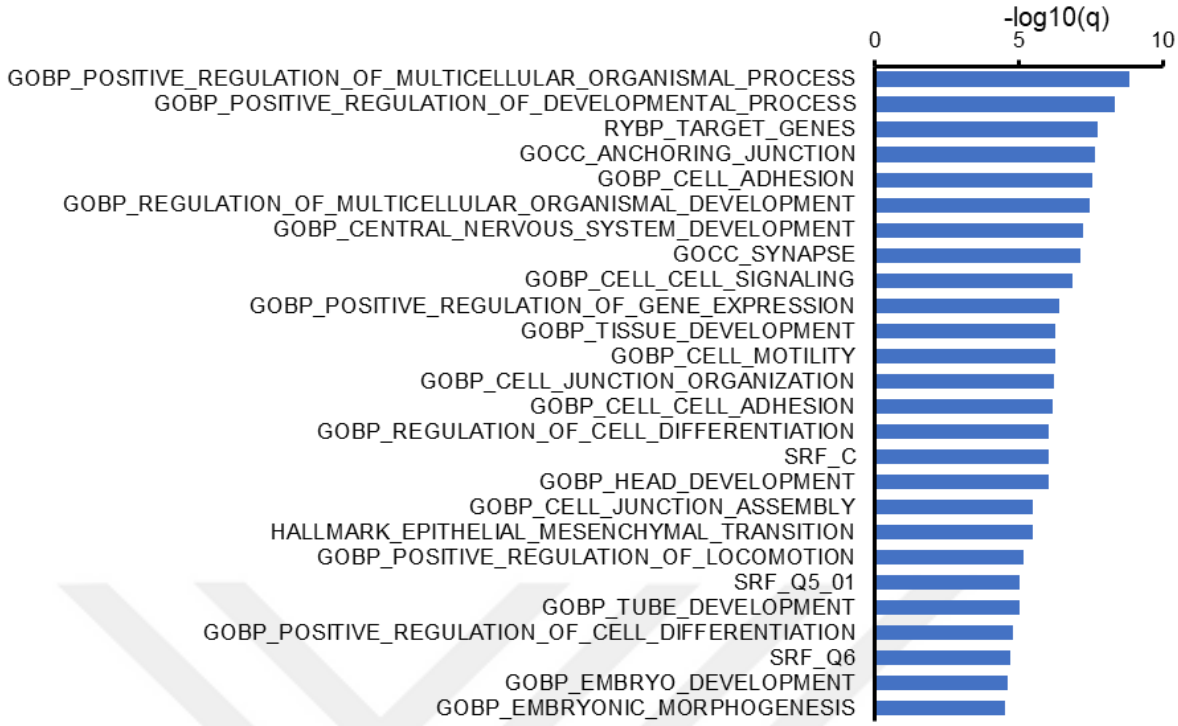

Figure 3.21. A) Gene ontology analysis for differentially upregulated genes upon USP22 knockout. Genesets related to pluripotency network were highlighted in red box. B) Gene ontology analysis for differentially downregulated genes upon USP22 knockout.

We next specifically addressed whether pluripotency related genes were upregulated upon USP22 knockout by performing gene set enrichment analysis (GSEA). Although USP22 loss did not increase reprogramming efficiency at day 6 of reprogramming, upregulated genes by USP22 loss were enriched in pluripotency related geneset (Figure 3.22). Similarly, downregulated genes by USP22 loss were enriched in fibroblast-related geneset (Figure 3.23). This GSEA result showed that USP22 loss enables cells to transcriptionally adapt to reprogramming more than control cells.

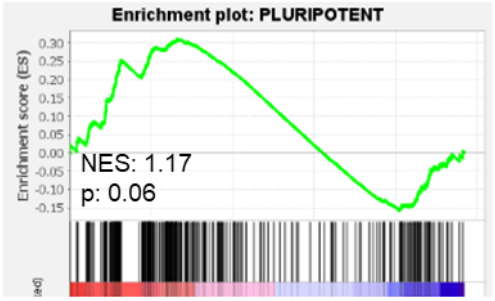

Figure 3.22. GSEA results for pluripotency-related genesets upon USP22 loss during reprogramming.

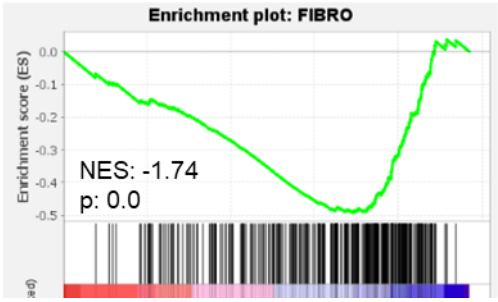

Figure 3.23. GSEA results for fibroblast-related genesets upon USP22 loss during reprogramming.

As a proof-of-concept, we quantified the expression levels of endogenous SOX2 levels during reprogramming upon USP22 loss and showed that it is upregulated 2-3-fold compared to non-targeting gRNA expressing cells at day 6, 9 and 12 of reprogramming (Figure 3.24). This time course gene expression analysis suggests that USP22 loss primes fibroblasts to reprogramming efficiently by re-activating endogenous pluripotency network.

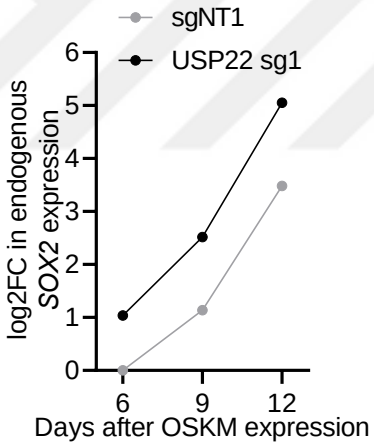

Figure 3.24. Fold change in the expression level of endogenous SOX2 upon USP22 compared to control during reprogramming. Normalized to day6 gNT1 expressing cells.

As the fibroblast-related geneset was negatively enriched in USP22 knockout cells during reprogramming, I hypothesized that USP22 loss may downregulate TGF-β signaling target genes to enhance reprogramming. Previous studies have shown that suppression of TGF-beta signaling can increase reprogramming efficiency (Ichida et al., 2009). To test this hypothesis, I reprogrammed cells in the absence of exogenous TGF-β added to the culture medium and observed that the USP22 knockout with 2 out of 3 guides did not increase reprogramming efficiency (Figure 3.25). To further explore this idea, I performed experiments using 2 different TGF-β inhibitors to ask whether TGF-β inhibition would have an additive

effect on reprogramming with USP22 loss (Figure 3.26). The results indicated that TGF-beta inhibitors did have an additive effect on the number of Tra-1-60-positive colonies when combined with USP22 gRNAs. These results suggest that the USP22 reprogramming phenotype is unlikely to be due to the regulation of TGF-beta signaling or its downstream targets.

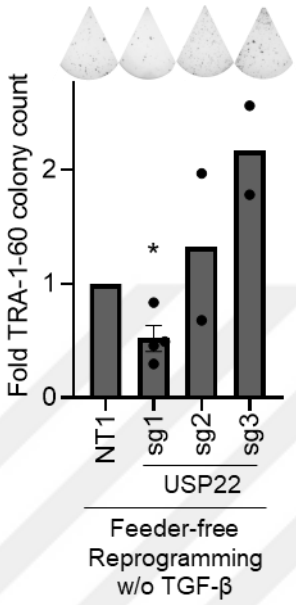

Figure 3.25. Fold change in the number of TRA-1-60 positive colonies compared to NT1 gRNA expressing cells.

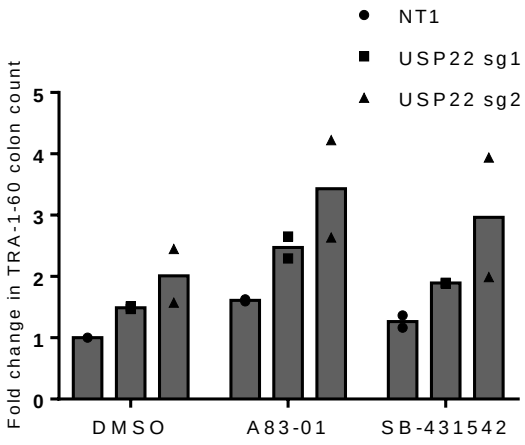

Figure 3.26. Fold change in the number of TRA-1-60 positive colonies compared to NT1 gRNA expressing cells treated with DMSO.

3.7.Characterization of USP22 knockout iPSCs

To investigate the effect of USP22 loss on human stem cell pluripotency, I picked and

expanded individual iPSC colonies generated from Cas9 and USP22 gRNA expressing fibroblasts (Figure 3.27). After several passages, western blot of whole cell lysates was performed to detect global USP22 protein levels. Interestingly, all individual clones generated from USP22 gRNA expressing cells lacked USP22 expression (Figure 3.28). This result indicates since full USP22 knockout could be expanded as iPSCs, USP22 loss does not prevent acquisition or maintenance of pluripotency.

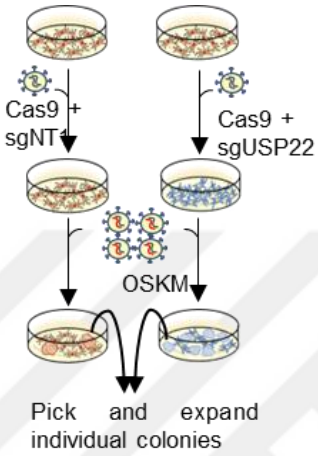

Figure 3.27. Schematic representation of generating USP22 knockout iPSC clones.

Figure 3.28. Western blot image showing USP22 protein levels in iPSCs generated from Cas9 and USP22 targeting gRNA expressing fibroblasts. Tubulin was used as a loading control.

iPSC clones generated from gRNA expressing cells were derived from lentivirally expressing OSKM factors which could confound any investigation of USP22's role in differentiation. This is because it has been reported that lentiviral OSKM may not be efficiently silenced and thereby prevent proper differentiation. To overcome this potential issue, I transduced an episomally generated iPSC cell line with Cas9 and USP22 gRNA to generate transgene-free USP22 knockout lines (Figure 3.29). After puromycin selection, serial dilutions were performed to get one iPSC in one well to isolate and expanded as single clones. Western blot of selected single iPSC clones after CRISPR-Cas9 expression showed that USP22 KO clones lacked the expression USP22 protein (Figure 3.30).

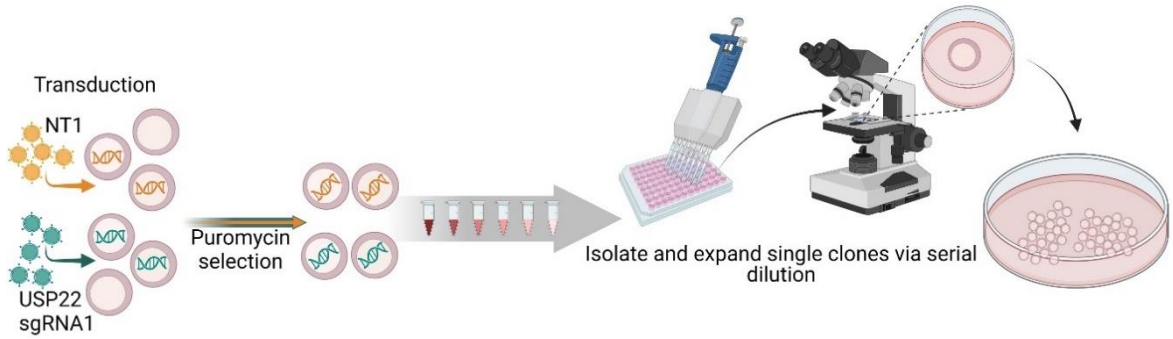

Figure 3.29. Schematic representation of generating single clone USP22 knockout iPSC colonies.

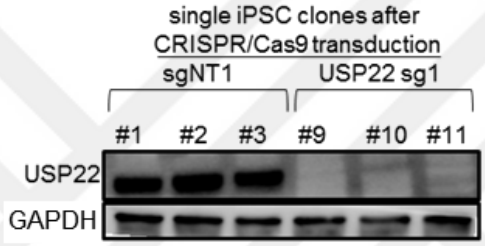

Figure 3.30. Western blot image showing USP22 protein levels after in iPSC clones generated from Cas9 and USP22 targeting gRNA expressing iPSCs. GAPDH was used as a loading control.

To characterize the effect of USP22 knockout on markers of the undifferentiated state in human iPSCs, we performed immunofluorescence analysis using NANOG and OCT4 antibodies (Figure 3.31). USP22 knockout clones displayed similar patterns and expression levels of these pluripotency markers compared to a control clone. Additionally, we performed karyotyping analysis of metaphases to detect chromosomal abnormalities. We detected normal karyotypes for all tested clones (Figure 3.32). To test the pluripotent stem cell differentiation capacity, we subjected each clone to *in vivo* differentiation by teratoma formation assay and observed cells from all three germ layers in sections (Figure 3.33). These results show that USP22 knockout iPSC lines are pluripotent.

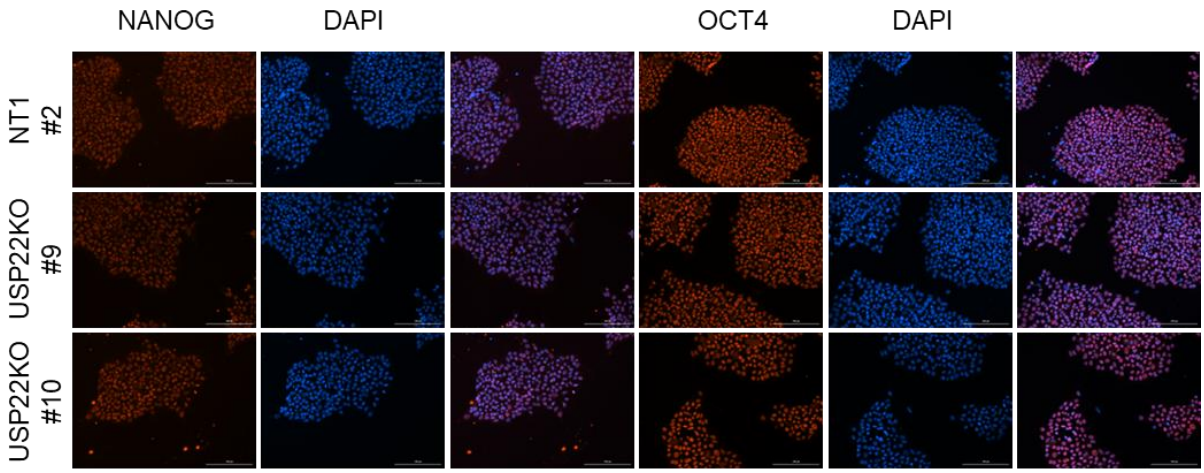

Figure 3.31. Immunofluorescence images of indicated clones for the expression of NANOG and OCT4. DAPI was used to stain nuclei.

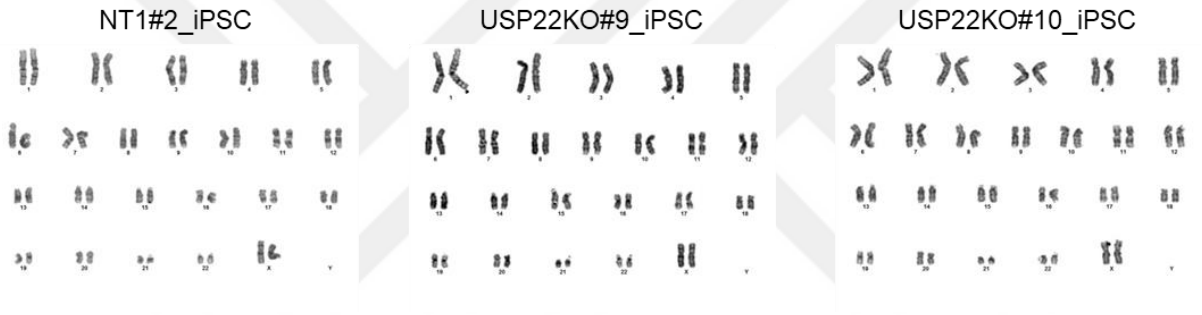

Figure 3.32. Karyotyping analysis of indicated clones.

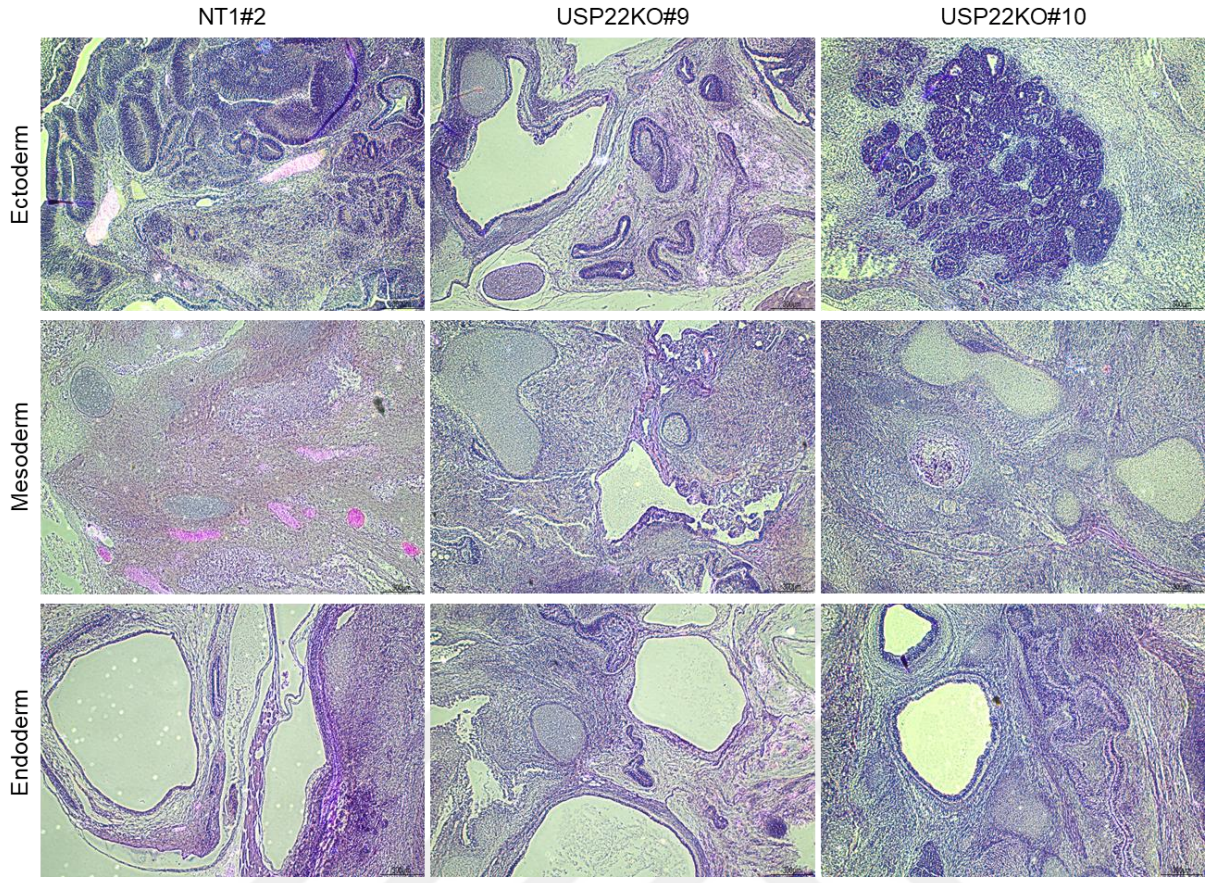

Figure 3.33. H&E staining sections of teratomas generated by USP22 knockout iPSCs show three germ layer differentiation capacities of each clone.

3.8.USP22 loss prevents robust exit from pluripotency.

To understand if USP22 loss has any impact on differentiation capacity of PSCs, I performed an in vitro differentiation assay to three germ layers via embryoid body formation (Figure 3.34). After 6 days in the culture, total RNA was extracted and RT-qPCR was performed for pluripotency (POU5F1, SOX2), mesoderm (TBXT, EOMES), endoderm (SOX17) and ectoderm (PAX6) markers (Figure 3.35). Compared to NT1 expressing control clone, USP22 knockout iPSC clones showed increased OCT4 and SOX2 expression at this time-point. Whereas during embryoid body differentiation, USP22 knockout resulted in decrease in mesoderm and endoderm markers up to 0.2-fold compared to control iPSCs. This result suggests that USP22 is required for efficient repression of pluripotency factors such as Oct4 and Sox2 during early differentiation.

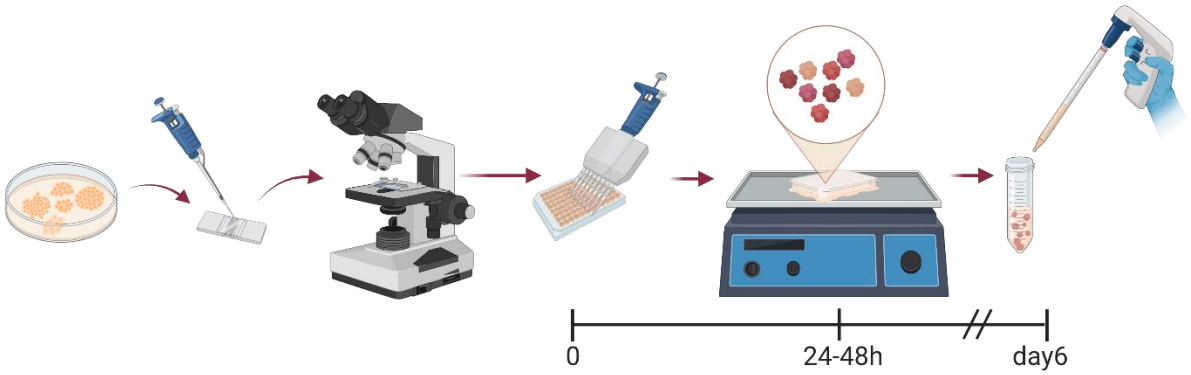

Figure 3.34. Schematic representation of embryoid body formation assay.

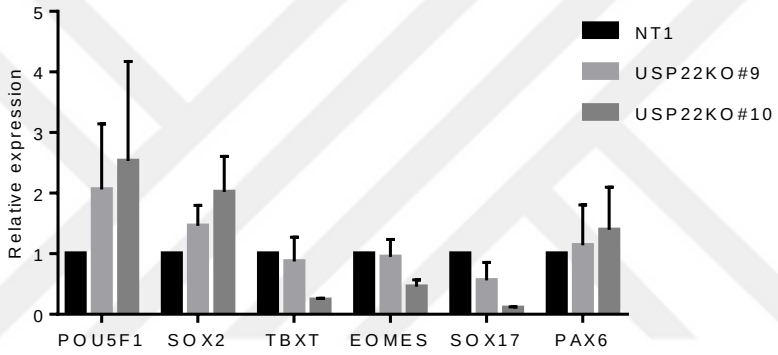

Figure 3.35. RT-qPCR analysis of indicated clones with several marker expression on day 6 of EB differentiation. Normalized to gNT1 expressing clone.

After observing differentiation defects in the embryoid body formation assay, we hypothesized that USP22 loss may impair TSC induction as it upregulates the endogenous SOX2 levels. As we observed an exit from pluripotency defect in USP22 KO clones during EB differentiation, we next wished to assess this phenotype in an alternative context. To address this, we first converted primed iPSCs into naive iPSCs (Figure 3.36 and 3.37). Then, these naive iPSCs were induced to differentiate towards TSCs using a 6 day protocol. Interestingly, we observed that in USP22 KO iPSCs, pluripotency markers SOX2 and OCT4 were not downregulated to the same extent as in control cells (Figure 3.38 and 3.39). These markers decreased around 0.05-fold in control cells whereas in USP22 knockout iPSCs retained around 0.2-fold compared to NT1 expressing iPSC. The deficiency in pluripotency exit upon USP22 loss was accompanied by defects in TSC differentiation as revealed by lower expression levels of trophoblast marker genes such as *TP63, GATA2* and *GATA3* (Figure 3.40 and 3.41). While these markers were robustly induced in control cells, USP22 knockout displayed 20-fold less

expression. These results suggest that USP22 is necessary for successful TSC induction from naive iPSCs by lowering the expression levels of the pluripotency network.

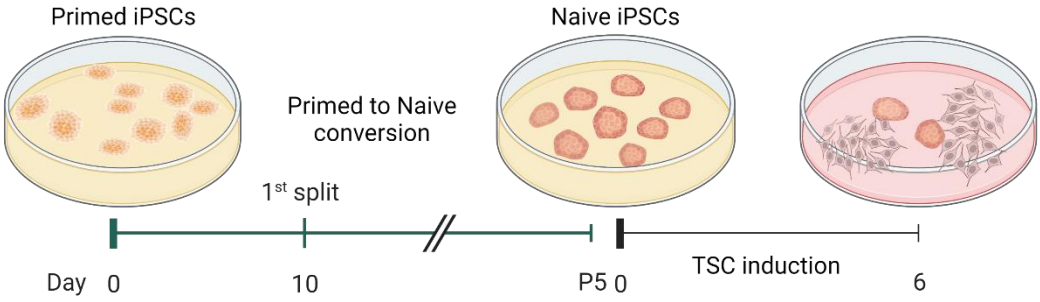

Figure 3.36. Schematic representation of TSC induction from primed iPSCs.

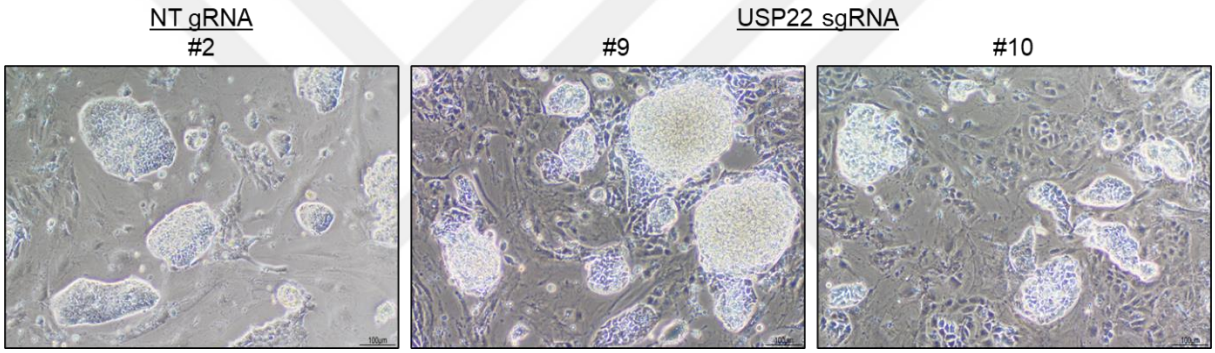

Figure 3.37. Bright field images of naive iPSCs

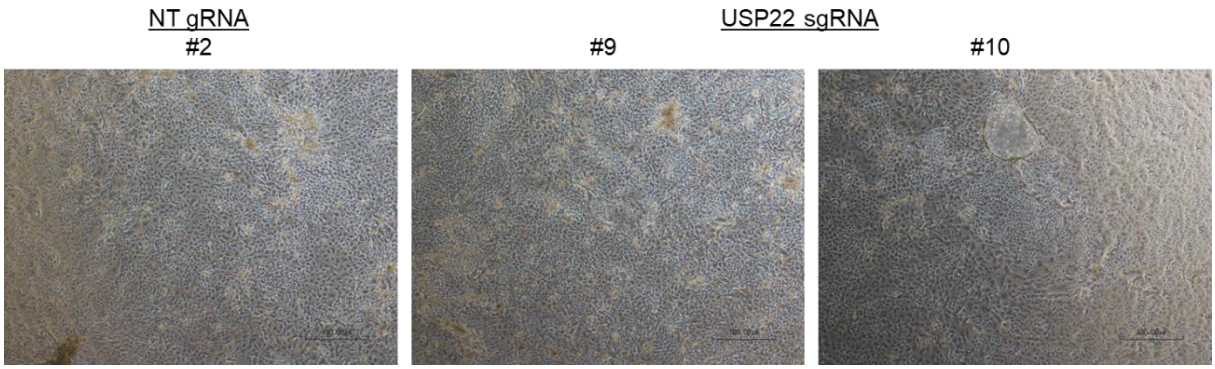

Figure 3.38. Bright field images of TSCs.

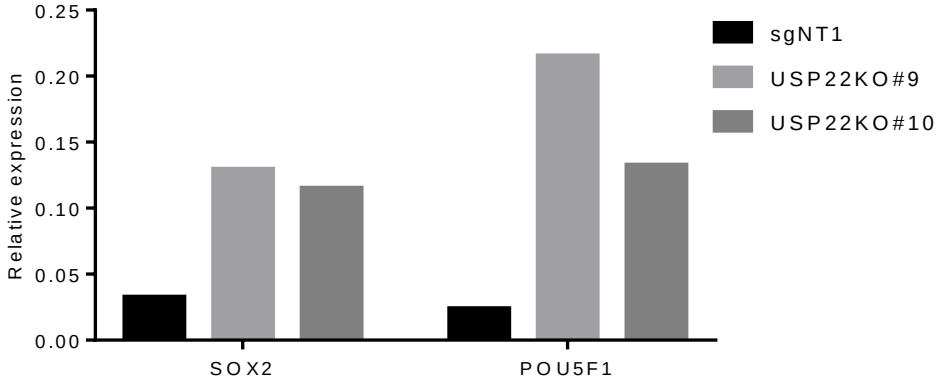

Figure 3.39. Fold change in expression levels of pluripotency markers relative to naive precursors of each clone.

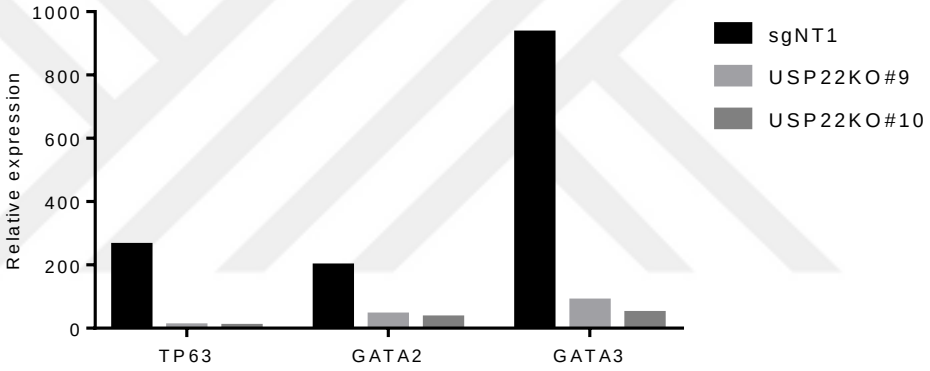

Figure 3.40. Fold change in expression levels of TSC markers relative to naive precursors of each clone.

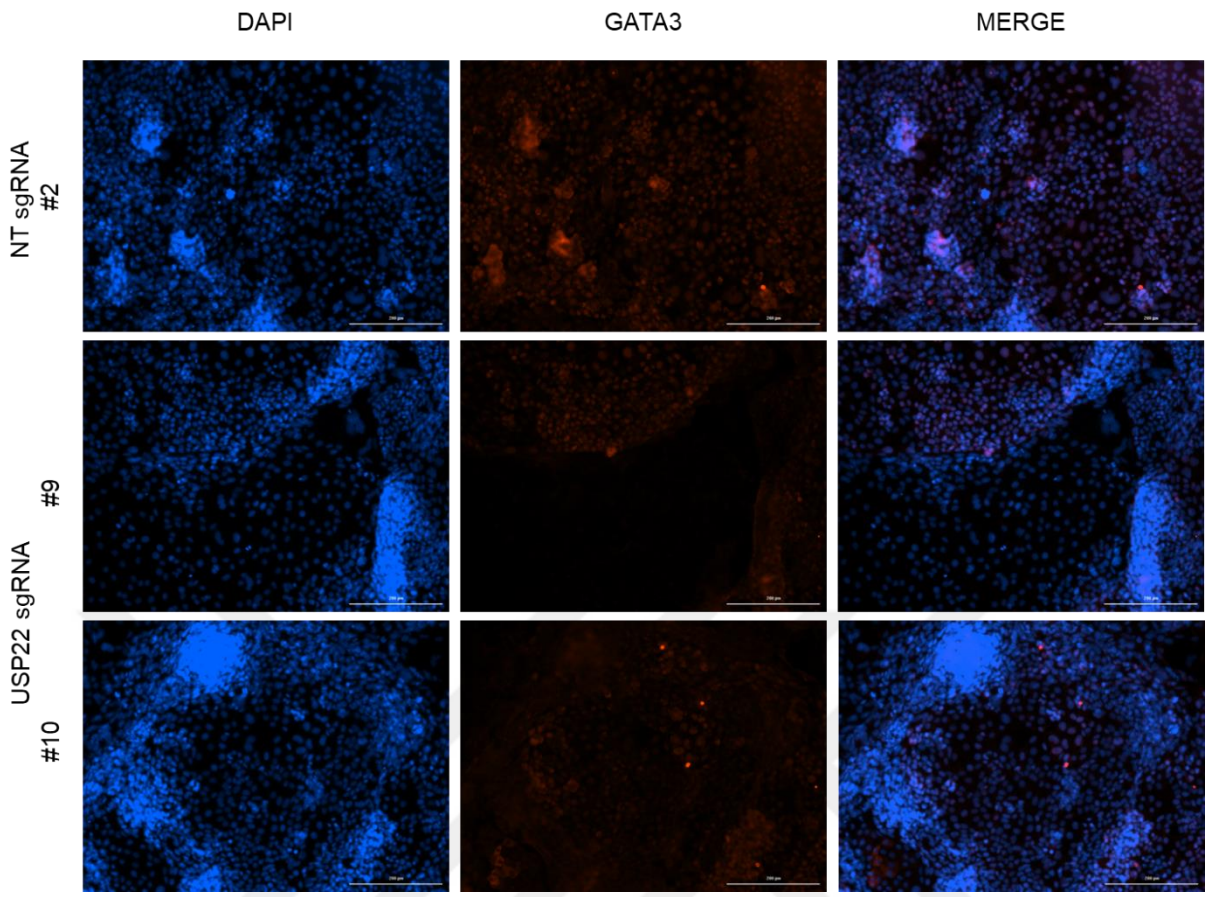

Figure 3.41. Immunofluorescence images of USP22 knockout TSCs for GATA3. (Scale: 200µm)

Chapter 4

DISCUSSION

Reprogramming consists of three stages, namely initiation, maturation, and maintenance. With chemical and Cas9-based screening, we can identify chromatin modifiers that may affect reprogramming and pluripotency at different time intervals. Our focused CRISPR-Cas9 screen identified previously known barriers to reprogramming including DNMT3A and EP300 (Ebrahimi et al., 2019b; Guo et al., 2013; Mikkelsen et al., 2008) at the maturation stage of reprogramming. DNA methylation was shown to be a barrier to reprogramming by various studies (Chen et al., 2015; Di Stefano et al., 2016; Gao et al., 2013). Additionally, CBP/EP300 bromodomains are barriers to reprogramming (Ebrahimi et al.,2019). This screen also identified a novel barrier to reprogramming, USP22 which was validated and subsequently analyzed in detail in this thesis. In the light of the articles, we have published before, we observed that this effect, which we saw at the end of reprogramming, did not appear at the initial stage when we performed the TRA-1-60 conjugated flow cytometry experiment to test precisely which phase the phenotype began to be reflected. As the increase in reprogramming efficiency may also be related to the increase in proliferation, CTG assay testing was performed on day 6 to check for this effect. We validated USP22's effect on reprogramming independent of the fibroblast line and using a different OSKM delivery method. Additionally, the effect of USP22 loss is additive with theDOT1L inhibition, enhancing the total efficiency by around 10-fold. These results are encouraging as novel inhibitors of the USP family are being developed (Alam &Atanassov, 2022; Morgan et al., 2022; Pei et al., 2022; Turnbull et al., 2017). We tested a cyclic peptide inhibitor of USP22 during reprogramming, previously reported to affect H2B ubiquitination (Appendix 1). However, in my hands, this inhibitor did not increase the global H2B ubiquitin levels in HEK 293T cells (Appendix 1). A complete knockout of USP22 did not increase the global H2B ubiquitin levels, this result is inconclusive as to whether the inhibitor was functional or not. When the USP22 inhibitor was used during reprogramming, we did not detect any change in reprogramming efficiency. This is as expected because catalytically dead USP22 could still rescue the knockout phenotype on reprogramming. I believe that USP22 selective degradation would increase the efficiency of small molecule-mediated reprogramming approaches (Guan et al., 2022b; Liuyang et al., 2023). At the same time, inhibition of possible protein interactions and functions of USP22 may provide insight into the mechanism of the effect on pluripotency. Interestingly, USP22's catalytic function and its involvement in the SAGA complex are not barriers to reprogramming. I speculate that USP22's zinc-finger domain is a barrier to reprogramming as this domain is

involved with protein-protein interactions. To address this, further experiments with zinc-finger domain deleted USP22 overexpression is necessary in USP22 knockout background to observe if this is the case.

Our CRISPR-Cas9 results of ATXN7L3 and ENY2 knockouts are encouraging as neither of these USP22 interaction partners are a barrier to reprogramming. Oppositely, ENY2 knockout has a detrimental impact on iPSC generation which could be due to its involvement in TREX complex-mediated RNA export (Jani et al., 2012; Kopytova et al., 2010). As these are the negative results, I did not perform these knockout experiments in USP22 knockout background. RNA-seq was performed on day 6 of reprogramming when reprogramming efficiency is not affected by USP22 loss. RNA-seq revealed gene sets such as SOX2, MYC, and SALL4-targets were upregulated whereas EMT, development, and differentiation-related genesets were downregulated. This RNA-seq and the following functional assays point to a model for USP22's role in differentiation and reprogramming in which USP22 suppresses the expression of endogenous SOX2 (Figure 4.1). USP22 loss upregulates SOX2 levels during reprogramming and fails to efficiently suppress SOX2 expression during differentiation. To show if the endogenous SOX2 levels are important in these cell fate decisions, shRNA mediated SOX2 knockdown could be performed in the USP22 knockout background during reprogramming and differentiation. Further studies are necessary to show how USP22 knockout acts to upregulate SOX2 levels mechanistically independent of its catalytic function.

Previous work has established that USP22 binds to SOX2 promoter to regulate its expression through H2B deubiquitination (Sussman et al., 2013). However, our results showed that catalytically dead USP22 could still rescue the USP22 knockout phenotype concerning reprogramming. Therefore, it is likely that USP22 regulates SOX2 expression in a deubiquitinase function-independent manner. To address this, SOX2 expression levels could be assessed when USP22catalytic dead mutant is overexpressed and compared to wild-type expression. If USP22 catalytic dead mutant could still rescue endogenous SOX2 levels to wild-type levels, that would suggest USP22 regulates SOX2 expression by binding to SOX2 promoter and acts as a repressor. To show this interaction, USP22 ChIP should be performed to see if USP22 binds to endogenous SOX2 promoter. Additionally, ChIP for USP22 catalytic dead mutant would be meaningful to see if USP22 still occupies the SOX2 promoter to suppress its expression. From a different perspective, the reduced suppression of OCT4 gene expression in USP22 knockout cells in embryoid body formation assay differentiation experiments, together with the SOX2 data, can only be used to explain its effect on pluripotency in general.

USP22 deletion is embryonic lethal in mice (Koutelou et al., 2019; Wang et al.,2021), and it causes defects in placental and kidney vascularization. Although teratomas derived from USP22 KO – iPSCs contained cells representative of all three germ layers in USP22 knockout

iPSCs, embryoid body formation assay indicated mesoderm and endoderm differentiation defects in one clone of USP22 knockouts. Additionally, TSC differentiation from naive iPSCs showed that USP22 loss causes problems in pluripotency exit as revealed by the inability to effectively downregulate pluripotency markers such as OCT4 and SOX2. Further experiments are needed to show which kind of TSC derivatives are most affected by USP22 loss and whether this phenotype is related to developmental defects observed in the mouse. It can be tested whether the possible effect in humans is similar to the mouse model by targeting differentiation into subtypes responsible for placenta and vascularization. Altogether, differentiation experiments suggested that embryonic lethality observed in mice may have a counterpart in early human development. To address this, early embryogenesis could be mimicked by recently developed models such as blastoid and gastruloid (Khoei et al., 2022; Ghimire et al., 2021). If there are defects in certain lineage commitments in USP22 knockout blastoids or gastruloids, this defect can be compared to developmental defects in mice development.

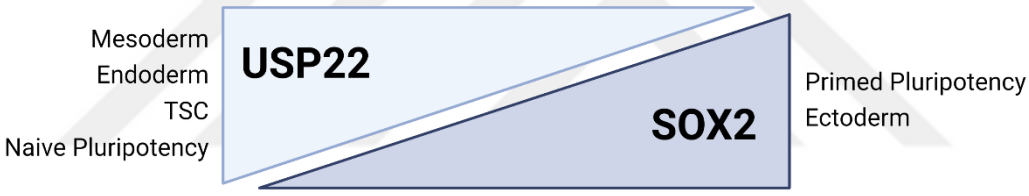

Figure 4.1. Working model of USP22's role in reprogramming and differentiation.

Chapter 5

REFERENCES

Aarts, M., Georgilis, A., Beniazza, M., Beolchi, P., Banito, A., Carroll, T., Kulisic, M., Kaemena, D. F., Dharmalingam, G., Martin, N., Reik, W., Zuber, J., Kaji, K., Chandra, T., & Gil, J. (2017). Coupling shRNA screens with single-cell RNA-seq identifies a dual role for mTOR in reprogramming-induced senescence. *Genes & Development*, *31*(20), 2085–2098. https://doi.org/10.1101/gad.297796.117

Akbari, S., Sevinç, G. G., Ersoy, N., Basak, O., Kaplan, K., Sevinç, K., Ozel, E., Sengun, B., Enustun, E., Ozcimen, B., Bagriyanik, A., Arslan, N., Önder, T. T., & Erdal, E. (2019). Robust, Long-Term Culture of Endoderm-Derived Hepatic Organoids for Disease Modeling. *Stem Cell Reports*, *13*(4), 627–641. https://doi.org/10.1016/j.stemcr.2019.08.007

Ao, N., Liu, Y., Feng, H., Bian, X., Li, Z., Gu, B., Zhao, X., & Liu, Y. (2014). Ubiquitin-Specific Peptidase USP22 Negatively Regulates the STAT Signaling Pathway by Deubiquitinating SIRT1. *Cellular Physiology and Biochemistry*, *33*(6), 1863–1875. https://doi.org/10.1159/000362964

Arabacı, D. H., Terzioğlu, G., Bayırbaşı, B., & Önder, T. T. (2020). Going up the hill: chromatin-based barriers to epigenetic reprogramming. *The FEBS Journal*, *n/a*(n/a). https://doi.org/https://doi.org/10.1111/febs.15628

Armour, S. M., Bennett, E. J., Braun, C. R., Zhang, X.-Y., McMahon, S. B., Gygi, S. P., Harper, J. W., & Sinclair, D. A. (2013). A High-Confidence Interaction Map Identifies SIRT1 as a Mediator of Acetylation of USP22 and the SAGA Coactivator Complex. *Molecular and Cellular Biology*, *33*(8), 1487–1502. https://doi.org/10.1128/MCB.00971-12

Atanassov, B. S., Evrard, Y. A., Multani, A. S., Zhang, Z., Tora, L., Devys, D., Chang, S., & Dent, S. Y. R. (2009). Gcn5 and SAGA Regulate Shelterin Protein Turnover and Telomere Maintenance. *Molecular Cell*, *35*(3), 352–364. https://doi.org/10.1016/j.molcel.2009.06.015

Baptista, T., Grünberg, S., Minoungou, N., Koster, M. J. E., Timmers, H. T. M., Hahn, S., Devys, D., & Tora, L. (2017). SAGA Is a General Cofactor for RNA Polymerase II Transcription. *Molecular Cell*, *68*(1), 130-143.e5. https://doi.org/10.1016/j.molcel.2017.08.016

Blackledge, N. P., Farcas, A. M., Kondo, T., King, H. W., McGouran, J. F., Hanssen, L. L. P., Ito, S., Cooper, S., Kondo, K., Koseki, Y., Ishikura, T., Long, H. K., Sheahan, T. W., Brockdorff, N., Kessler, B. M., Koseki, H., & Klose, R. J. (2014). Variant PRC1 complex-dependent H2A ubiquitylation drives PRC2 recruitment and polycomb domain formation. *Cell*, *157*(6), 1445–1459. https://doi.org/10.1016/j.cell.2014.05.004

Bonnet, J., Romier, C., Tora, L., & Devys, D. (2008). Zinc-finger UBPs: regulators of deubiquitylation. *Trends in Biochemical Sciences*, *33*(8), 369–375. https://doi.org/https://doi.org/10.1016/j.tibs.2008.05.005

Bonnet, J., Wang, C.-Y., Baptista, T., Vincent, S. D., Hsiao, W.-C., Stierle, M., Kao, C.-F., Tora, L., & Devys, D. (2014). The SAGA coactivator complex acts on the whole transcribed genome and is required for RNA polymerase II transcription. *Genes & Development*, *28*(18), 1999–2012.

Borkent, M., Bennett, B. D., Lackford, B., Bar-Nur, O., Brumbaugh, J., Wang, L., Du, Y., Fargo, D. C., Apostolou, E., Cheloufi, S., Maherali, N., Elledge, S. J., Hu, G., & Hochedlinger, K. (2016). A Serial shRNA Screen for Roadblocks to Reprogramming Identifies the Protein Modifier SUMO2. *Stem Cell Reports*, *6*(5), 704–716. https://doi.org/10.1016/j.stemcr.2016.02.004

Brumbaugh, J., Di Stefano, B., & Hochedlinger, K. (2019). Reprogramming: identifying the mechanisms that safeguard cell identity. *Development*, *146*(23), dev182170. https://doi.org/10.1242/dev.182170

Buganim, Y., Faddah, D. A., & Jaenisch, R. (2013). Mechanisms and models of somatic cell reprogramming. *Nature Reviews. Genetics*, *14*(6), 427–439. https://doi.org/10.1038/nrg3473

Cacchiarelli, D., Trapnell, C., Ziller, M. J., Soumillon, M., Cesana, M., Karnik, R., Donaghey, J., Smith, Z. D., Ratanasirintrawoot, S., Zhang, X., Ho Sui, S. J., Wu, Z., Akopian, V., Gifford, C. A., Doench, J., Rinn, J. L., Daley, G. Q., Meissner, A., Lander, E. S., & Mikkelsen, T. S. (2015). Integrative Analyses of Human Reprogramming Reveal Dynamic Nature of Induced Pluripotency. *Cell*, *162*(2), 412–424. https://doi.org/10.1016/j.cell.2015.06.016

Camp, J. G., Badsha, F., Florio, M., Kanton, S., Gerber, T., Wilsch-Bräuninger, M., Lewitus, E., Sykes, A., Hevers, W., Lancaster, M., Knoblich, J. A., Lachmann, R., Pääbo, S., Huttner, W. B., & Treutlein, B. (2015). Human cerebral organoids recapitulate gene expression programs of fetal neocortex development. *Proceedings of the National*

Academy of Sciences of the United States of America, *112*(51), 15672–15677. https://doi.org/10.1073/pnas.1520760112

Campagne, A., Lee, M.-K., Zielinski, D., Michaud, A., Le Corre, S., Dingli, F., Chen, H., Shahidian, L. Z., Vassilev, I., Servant, N., Loew, D., Pasmant, E., Postel-Vinay, S., Wassef, M., & Margueron, R. (2019). BAP1 complex promotes transcription by opposing PRC1-mediated H2A ubiquitylation. *Nature Communications*, *10*(1), 348. https://doi.org/10.1038/s41467-018-08255-x

Chan, Y.-S., Göke, J., Ng, J.-H., Lu, X., Gonzales, K. A. U., Tan, C.-P., Tng, W.-Q., Hong, Z.-Z., Lim, Y.-S., & Ng, H.-H. (2013). Induction of a human pluripotent state with distinct regulatory circuitry that resembles preimplantation epiblast. *Cell Stem Cell*, *13*(6), 663–675. https://doi.org/10.1016/j.stem.2013.11.015

Chandrasekharan, M. B., Huang, F., & Sun, Z.-W. (2009). Ubiquitination of histone H2B regulates chromatin dynamics by enhancing nucleosome stability. *Proceedings of the National Academy of Sciences*, *106*(39), 16686 LP – 16691. https://doi.org/10.1073/pnas.0907862106

Cheloufi, S., Elling, U., Hopfgartner, B., Jung, Y. L., Murn, J., Ninova, M., Hubmann, M., Badeaux, A. I., Euong Ang, C., Tenen, D., Wesche, D. J., Abazova, N., Hogue, M., Tasdemir, N., Brumbaugh, J., Rathert, P., Jude, J., Ferrari, F., Blanco, A., … Hochedlinger, K. (2015). The histone chaperone CAF-1 safeguards somatic cell identity. *Nature*, *528*(7581), 218–224. https://doi.org/10.1038/nature15749

Chen, J., Gao, Y., Huang, H., Xu, K., Chen, X., Jiang, Y., Li, H., Gao, S., Tao, Y., Wang, H., Zhang, Y., Wang, H., Cai, T., & Gao, S. (2015). The Combination of Tet1 with Oct4 Generates High-Quality Mouse-Induced Pluripotent Stem Cells. *STEM CELLS*, *33*(3), 686–698. https://doi.org/https://doi.org/10.1002/stem.1879

Cheon, Y., Kim, H., Park, K., Kim, M., & Lee, D. (2020). Dynamic modules of the coactivator SAGA in eukaryotic transcription. *Experimental & Molecular Medicine*, *52*(7), 991–1003. https://doi.org/10.1038/s12276-020-0463-4

Choi, J., Costa, M. L., Mermelstein, C. S., Chagas, C., Holtzer, S., & Holtzer, H. (1990). MyoD converts primary dermal fibroblasts, chondroblasts, smooth muscle, and retinal pigmented epithelial cells into striated mononucleated myoblasts and multinucleated myotubes. *Proceedings of the National Academy of Sciences of the United States of America*, *87*(20), 7988–7992. https://doi.org/10.1073/pnas.87.20.7988

Chronis, C., Fiziev, P., Papp, B., Butz, S., Bonora, G., Sabri, S., Ernst, J., & Plath, K. (2017). Cooperative Binding of Transcription Factors Orchestrates Reprogramming. *Cell*, *168*(3), 442-459.e20. https://doi.org/10.1016/j.cell.2016.12.016

Cossec, J.-C., Theurillat, I., Chica, C., Búa Aguín, S., Gaume, X., Andrieux, A., Iturbide, A., Jouvion, G., Li, H., Bossis, G., Seeler, J.-S., Torres-Padilla, M.-E., & Dejean, A. (2018). SUMO Safeguards Somatic and Pluripotent Cell Identities by Enforcing Distinct Chromatin States. *Cell Stem Cell*, *23*(5), 742-757.e8. https://doi.org/https://doi.org/10.1016/j.stem.2018.10.001

Cowan, C. A., Atienza, J., Melton, D. A., & Eggan, K. (2005). Nuclear reprogramming of somatic cells after fusion with human embryonic stem cells. *Science (New York, N.Y.)*, *309*(5739), 1369–1373. https://doi.org/10.1126/science.1116447

Cowan, C. A., Klimanskaya, I., McMahon, J., Atienza, J., Witmyer, J., Zucker, J. P., Wang, S., Morton, C. C., McMahon, A. P., Powers, D., & Melton, D. A. (2004). Derivation of embryonic stem-cell lines from human blastocysts. *The New England Journal of Medicine*, *350*(13), 1353–1356. https://doi.org/10.1056/NEJMsr040330

Cyranoski, D. (2018). "Reprogrammed" stem cells approved to mend human hearts for the first time. In *Nature* (Vol. 557, Issue 7707, pp. 619–620). https://doi.org/10.1038/d41586-018-05278-8

Dahéron, L., Opitz, S. L., Zaehres, H., Lensch, M. W., Andrews, P. W., Itskovitz-Eldor, J., & Daley, G. Q. (2004). LIF/STAT3 signaling fails to maintain self-renewal of human embryonic stem cells. *Stem Cells (Dayton, Ohio)*, *22*(5), 770–778. https://doi.org/10.1634/stemcells.22-5-770

Di Stefano, B., Collombet, S., Jakobsen, J. S., Wierer, M., Sardina, J. L., Lackner, A., Stadhouders, R., Segura-Morales, C., Francesconi, M., Limone, F., Mann, M., Porse, B., Thieffry, D., & Graf, T. (2016). C/EBPα creates elite cells for iPSC reprogramming by upregulating Klf4 and increasing the levels of Lsd1 and Brd4. *Nature Cell Biology*, *18*(4), 371–381. https://doi.org/10.1038/ncb3326

Do, J. T., & Schöler, H. R. (2006). Cell-cell fusion as a means to establish pluripotency. *Ernst Schering Research Foundation Workshop*, *60*, 35–45. https://doi.org/10.1007/3-540-31437-7_4

Dover, J., Schneider, J., Tawiah-Boateng, M. A., Wood, A., Dean, K., Johnston, M., & Shilatifard, A. (2002). Methylation of Histone H3 by COMPASS Requires Ubiquitination of Histone H2B by Rad6. *Journal of Biological Chemistry*, *277*(32), 28368–28371. http://www.jbc.org/content/277/32/28368.abstract

Duran Alonso, M. B., Lopez Hernandez, I., de la Fuente, M. A., Garcia-Sancho, J., Giraldez, F., & Schimmang, T. (2018). Transcription factor induced conversion of human fibroblasts towards the hair cell lineage. *PloS One*, *13*(7), e0200210. https://doi.org/10.1371/journal.pone.0200210

Durand, A., Bonnet, J., Fournier, M., Chavant, V., & Schultz, P. (2014). Mapping the Deubiquitination Module within the SAGA Complex. *Structure*, *22*(11), 1553–1559. https://doi.org/https://doi.org/10.1016/j.str.2014.07.017

Dye, B. R., Hill, D. R., Ferguson, M. A. H., Tsai, Y.-H., Nagy, M. S., Dyal, R., Wells, J. M., Mayhew, C. N., Nattiv, R., Klein, O. D., White, E. S., Deutsch, G. H., & Spence, J. R. (2015). In vitro generation of human pluripotent stem cell derived lung organoids. *ELife*, *4*. https://doi.org/10.7554/eLife.05098

Ebrahimi, A., Sevinç, K., Gürhan Sevinç, G., Cribbs, A. P., Philpott, M., Uyulur, F., Morova, T., Dunford, J. E., Göklemez, S., Arı, Ş., Oppermann, U., & Önder, T. T. (2019a). Bromodomain inhibition of the coactivators CBP/EP300 facilitate cellular reprogramming. *Nature Chemical Biology*, *15*(5), 519–528. https://doi.org/10.1038/s41589-019-0264-z

Ebrahimi, A., Sevinç, K., Gürhan Sevinç, G., Cribbs, A. P., Philpott, M., Uyulur, F., Morova, T., Dunford, J. E., Göklemez, S., Arı, Ş., Oppermann, U., & Önder, T. T. (2019b). Bromodomain inhibition of the coactivators CBP/EP300 facilitate cellular reprogramming. *Nature Chemical Biology*, *15*(5), 519–528. https://doi.org/10.1038/s41589-019-0264-z

Endoh, M., Endo, T. A., Endoh, T., Isono, K., Sharif, J., Ohara, O., Toyoda, T., Ito, T., Eskeland, R., Bickmore, W. A., Vidal, M., Bernstein, B. E., & Koseki, H. (2012). Histone H2A Mono-Ubiquitination Is a Crucial Step to Mediate PRC1-Dependent Repression of Developmental Genes to Maintain ES Cell Identity. *PLOS Genetics*, *8*(7), e1002774. https://doi.org/10.1371/journal.pgen.1002774

Evans, M. J., & Kaufman, M. H. (1981). Establishment in culture of pluripotential cells from mouse embryos. *Nature*, *292*(5819), 154–156. https://doi.org/10.1038/292154a0

Firas, J., Liu, X., Lim, S. M., & Polo, J. M. (2015). Transcription factor-mediated reprogramming: epigenetics and therapeutic potential. *Immunology and Cell Biology*, *93*(3), 284–289. https://doi.org/10.1038/icb.2015.5

FISCHBERG, M., GURDON, J. B., & ELSDALE, T. R. (1958). Nuclear Transplantation in Xenopus laevis. *Nature*, *181*(4606), 424. https://doi.org/10.1038/181424a0

Gafni, O., Weinberger, L., Mansour, A. A., Manor, Y. S., Chomsky, E., Ben-Yosef, D., Kalma, Y., Viukov, S., Maza, I., Zviran, A., Rais, Y., Shipony, Z., Mukamel, Z., Krupalnik, V., Zerbib, M., Geula, S., Caspi, I., Schneir, D., Shwartz, T., … Hanna, J. H. (2013). Derivation of novel human ground state naive pluripotent stem cells. *Nature*, *504*(7479), 282–286. https://doi.org/10.1038/nature12745

Gamper, A. M., Kim, J., & Roeder, R. G. (2009). The STAGA subunit ADA2b is an important regulator of human GCN5 catalysis. *Molecular and Cellular Biology*, *29*(1), 266–280. https://doi.org/10.1128/MCB.00315-08

Gao, Y., Chen, J., Li, K., Wu, T., Huang, B., Liu, W., Kou, X., Zhang, Y., Huang, H., Jiang, Y., Yao, C., Liu, X., Lu, Z., Xu, Z., Kang, L., Chen, J., Wang, H., Cai, T., & Gao, S. (2013). Replacement of Oct4 by Tet1 during iPSC Induction Reveals an Important Role of DNA Methylation and Hydroxymethylation in Reprogramming. *Cell Stem Cell*, *12*(4), 453–469. https://doi.org/10.1016/j.stem.2013.02.005

Gao, Y., Lin, F., Xu, P., Nie, J., Chen, Z., Su, J., Tang, J., Wu, Q., Li, Y., Guo, Z., Gao, Z., Li, D., Shen, J., Ge, S., Tsun, A., & Li, B. (2014). USP22 is a positive regulator of NFATc2 on promoting IL2 expression. *FEBS Letters*, *588*(6), 878–883. https://doi.org/https://doi.org/10.1016/j.febslet.2014.02.016

Garcez, P. P., Loiola, E. C., Madeiro da Costa, R., Higa, L. M., Trindade, P., Delvecchio, R., Nascimento, J. M., Brindeiro, R., Tanuri, A., & Rehen, S. K. (2016). Zika virus impairs growth in human neurospheres and brain organoids. *Science (New York, N.Y.)*, *352*(6287), 816–818. https://doi.org/10.1126/science.aaf6116

Ghimire, S., Van der Jeught, M., Neupane, J., Roost, M. S., Anckaert, J., Popovic, M., Van Nieuwerburgh, F., Mestdagh, P., Vandesompele, J., Deforce, D., Menten, B., Chuva de Sousa Lopes, S., De Sutter, P., & Heindryckx, B. (2018). Comparative analysis of naive, primed and ground state pluripotency in mouse embryonic stem cells originating from the same genetic background. *Scientific Reports*, *8*(1), 5884. https://doi.org/10.1038/s41598-018-24051-5

Ghimire, S., et al., (2021). Human gastrulation: The embryo and its models. *Developmental Biology*, 474, 100-108.

Ghosh, T. K., Aparicio-Sánchez, J. J., Buxton, S., Ketley, A., Mohamed, T., Rutland, C. S., Loughna, S., & Brook, J. D. (2018). Acetylation of TBX5 by KAT2B and KAT2A regulates heart and limb development. *Journal of Molecular and Cellular Cardiology*, *114*, 185–198. https://doi.org/10.1016/j.yjmcc.2017.11.013

Golipour, A., David, L., Liu, Y., Jayakumaran, G., Hirsch, C. L., Trcka, D., & Wrana, J. L. (2012). A Late Transition in Somatic Cell Reprogramming Requires Regulators Distinct from the Pluripotency Network. *Cell Stem Cell*, *11*(6), 769–782. https://doi.org/https://doi.org/10.1016/j.stem.2012.11.008

González, F., & Huangfu, D. (2016). Mechanisms underlying the formation of induced pluripotent stem cells. *Wiley Interdisciplinary Reviews. Developmental Biology*, *5*(1), 39–65. https://doi.org/10.1002/wdev.206

Guan, J., Wang, G., Wang, J., Zhang, Z., Fu, Y., Cheng, L., Meng, G., Lyu, Y., Zhu, J., Li, Y., Wang, Y., Liuyang, S., Liu, B., Yang, Z., He, H., Zhong, X., Chen, Q., Zhang, X., Sun, S., … Deng, H. (2022a). Chemical reprogramming of human somatic cells to pluripotent stem cells. *Nature*, *605*(7909), 325–331. https://doi.org/10.1038/s41586-022-04593-5

Guan, J., Wang, G., Wang, J., Zhang, Z., Fu, Y., Cheng, L., Meng, G., Lyu, Y., Zhu, J., Li, Y., Wang, Y., Liuyang, S., Liu, B., Yang, Z., He, H., Zhong, X., Chen, Q., Zhang, X., Sun, S., … Deng, H. (2022b). Chemical reprogramming of human somatic cells to pluripotent stem cells. *Nature*, *605*(7909), 325–331. https://doi.org/10.1038/s41586-022-04593-5

Guo, X., Liu, Q., Wang, G., Zhu, S., Gao, L., Hong, W., Chen, Y., Wu, M., Liu, H., Jiang, C., & Kang, J. (2013). microRNA-29b is a novel mediator of Sox2 function in the regulation of somatic cell reprogramming. *Cell Research*, *23*(1), 142–156. https://doi.org/10.1038/cr.2012.180

GURDON, J. B. (1960). The developmental capacity of nuclei taken from differentiating endoderm cells of Xenopus laevis. *Journal of Embryology and Experimental Morphology*, *8*, 505–526.

GURDON, J. B. (1962a). Adult frogs derived from the nuclei of single somatic cells. *Developmental Biology*, *4*, 256–273. https://doi.org/10.1016/0012-1606(62)90043-x

GURDON, J. B. (1962b). The developmental capacity of nuclei taken from intestinal epithelium cells of feeding tadpoles. *Journal of Embryology and Experimental Morphology*, *10*, 622–640.

Hanna, J., Carey, B. W., & Jaenisch, R. (2008). Reprogramming of somatic cell identity. *Cold Spring Harbor Symposia on Quantitative Biology*, *73*, 147–155. https://doi.org/10.1101/sqb.2008.73.025

Hanna, J., Cheng, A. W., Saha, K., Kim, J., Lengner, C. J., Soldner, F., Cassady, J. P., Muffat, J., Carey, B. W., & Jaenisch, R. (2010). Human embryonic stem cells with biological and epigenetic characteristics similar to those of mouse ESCs. *Proceedings of the National*

Academy of Sciences of the United States of America, *107*(20), 9222–9227. https://doi.org/10.1073/pnas.1004584107

Helmlinger, D., & Tora, L. (2017). Sharing the SAGA. *Trends in Biochemical Sciences*, *42*(11), 850–861. https://doi.org/10.1016/j.tibs.2017.09.001

Henry, K. W., Wyce, A., Lo, W.-S., Duggan, L. J., Emre, N. C. T., Kao, C.-F., Pillus, L., Shilatifard, A., Osley, M. A., & Berger, S. L. (2003). Transcriptional activation via sequential histone H2B ubiquitylation and deubiquitylation, mediated by SAGA-associated Ubp8. *Genes & Development*, *17*(21), 2648–2663. http://genesdev.cshlp.org/content/17/21/2648.abstract

Hernandez, C., Wang, Z., Ramazanov, B., Tang, Y., Mehta, S., Dambrot, C., Lee, Y.-W., Tessema, K., Kumar, I., Astudillo, M., Neubert, T. A., Guo, S., & Ivanova, N. B. (2018). Dppa2/4 Facilitate Epigenetic Remodeling during Reprogramming to Pluripotency. *Cell Stem Cell*, *23*(3), 396-411.e8. https://doi.org/10.1016/j.stem.2018.08.001

Hirsch, C. L., Akdemir, Z. C., Wang, L., Jayakumaran, G., Trcka, D., Weiss, A., Hernandez, J. J., Pan, Q., Han, H., Xu, X., Xia, Z., Salinger, A. P., Wilson, M., Vizeacoumar, F., Datti, A., Li, W., Cooney, A. J., Barton, M. C., Blencowe, B. J., … Dent, S. Y. R. (2015). Myc and SAGA rewire an alternative splicing network during early somatic cell reprogramming. *Genes and Development*, *29*(8), 803–816. https://doi.org/10.1101/gad.255109.114

Hirsch, C. L., Coban Akdemir, Z., Wang, L., Jayakumaran, G., Trcka, D., Weiss, A., Hernandez, J. J., Pan, Q., Han, H., Xu, X., Xia, Z., Salinger, A. P., Wilson, M., Vizeacoumar, F., Datti, A., Li, W., Cooney, A. J., Barton, M. C., Blencowe, B. J., … Dent, S. Y. R. (2015). Myc and SAGA rewire an alternative splicing network during early somatic cell reprogramming. *Genes & Development*, *29*(8), 803–816. https://doi.org/10.1101/gad.255109.114

Ho, L., Miller, E. L., Ronan, J. L., Ho, W. Q., Jothi, R., & Crabtree, G. R. (2011). EsBAF facilitates pluripotency by conditioning the genome for LIF/STAT3 signalling and by regulating polycomb function. *Nature Cell Biology*, *13*(8), 903–913. https://doi.org/10.1038/ncb2285

Hsu, P. L., Shi, H., Leonen, C., Kang, J., Chatterjee, C., & Zheng, N. (2019). Structural Basis of H2B Ubiquitination-Dependent H3K4 Methylation by COMPASS. *Molecular Cell*, *76*(5), 712-723.e4. https://doi.org/https://doi.org/10.1016/j.molcel.2019.10.013

Huang, Y., Zhang, H., Wang, L., Tang, C., Qin, X., Wu, X., Pan, M., Tang, Y., Yang, Z., Babarinde, I. A., Lin, R., Ji, G., Lai, Y., Xu, X., Su, J., Wen, X., Satoh, T., Ahmed, T.,

Malik, V., Qin, B. (2020). JMJD3 acts in tandem with KLF4 to facilitate reprogramming to pluripotency. *Nature Communications*, *11*(1), 5061. https://doi.org/10.1038/s41467-020-18900-z

Huangfu, D., Maehr, R., Guo, W., Eijkelenboom, A., Snitow, M., Chen, A. E., & Melton, D. A. (2008). Induction of pluripotent stem cells by defined factors is greatly improved by small-molecule compounds. *Nature Biotechnology*, *26*(7), 795–797. https://doi.org/10.1038/nbt1418

Ieda, M. (2013). Direct reprogramming into desired cell types by defined factors. *The Keio Journal of Medicine*, *62*(3), 74–82. https://doi.org/10.2302/kjm.2012-0017-re

Jang, S., Kang, C., Yang, H.-S., Jung, T., Hebert, H., Chung, K. Y., Kim, S. J., Hohng, S., & Song, J.-J. (2019). Structural basis of recognition and destabilization of the histone H2B ubiquitinated nucleosome by the DOT1L histone H3 Lys79 methyltransferase. *Genes & Development*, *33*(11–12), 620–625. https://doi.org/10.1101/gad.323790.118

Jani, D., Lutz, S., Hurt, E., Laskey, R. A., Stewart, M., & Wickramasinghe, V. O. (2012). Functional and structural characterization of the mammalian TREX-2 complex that links transcription with nuclear messenger RNA export. *Nucleic Acids Research*, *40*(10), 4562–4573. https://doi.org/10.1093/nar/gks059

Jedrusik, A. (2015). Making the first decision: lessons from the mouse. *Reproductive Medicine and Biology*, *14*(4), 135–150. https://doi.org/10.1007/s12522-015-0206-8

Jiang, Q., Huang, X., Hu, X., Shan, Z., Wu, Y., Wu, G., & Lei, L. (2020). Histone demethylase KDM6A promotes somatic cell reprogramming by epigenetically regulating the PTEN and IL-6 signal pathways. *Stem Cells (Dayton, Ohio)*, *38*(8), 960–972. https://doi.org/10.1002/stem.3188

Kim, D., Hong, A., Park, H. I., Shin, W. H., Yoo, L., Jeon, S. J., & Chung, K. C. (2017). Deubiquitinating enzyme USP22 positively regulates c-Myc stability and tumorigenic activity in mammalian and breast cancer cells. *Journal of Cellular Physiology*, *232*(12), 3664–3676. https://doi.org/10.1002/jcp.25841

Kim, E. J. Y., Anko, M.-L., Flensberg, C., Majewski, I. J., Geng, F.-S., Firas, J., Huang, D. C. S., van Delft, M. F., & Heath, J. K. (2018). BAK/BAX-Mediated Apoptosis Is a Myc-Induced Roadblock to Reprogramming. *Stem Cell Reports*, *10*(2), 331–338. https://doi.org/10.1016/j.stemcr.2017.12.019

Kim, K.-P., Choi, J., Yoon, J., Bruder, J. M., Shin, B., Kim, J., Arauzo-Bravo, M. J., Han, D., Wu, G., Han, D. W., Kim, J., Cramer, P., & Schöler, H. R. (2021). Permissive epigenomes

endow reprogramming competence to transcriptional regulators. *Nature Chemical Biology*, *17*(1), 47–56. https://doi.org/10.1038/s41589-020-0618-6

Klimanskaya, I., Chung, Y., Becker, S., Lu, S.-J., & Lanza, R. (2006). Human embryonic stem cell lines derived from single blastomeres. *Nature*, *444*(7118), 481–485. https://doi.org/10.1038/nature05142

Kobayashi, T., Iwamoto, Y., Takashima, K., Isomura, A., Kosodo, Y., Kawakami, K., Nishioka, T., Kaibuchi, K., & Kageyama, R. (2015). Deubiquitinating enzymes regulate Hes1 stability and neuronal differentiation. *The FEBS Journal*, *282*(13), 2411–2423. https://doi.org/10.1111/febs.13290

Koche, R. P., Smith, Z. D., Adli, M., Gu, H., Ku, M., Gnirke, A., Bernstein, B. E., & Meissner, A. (2011). Reprogramming factor expression initiates widespread targeted chromatin remodeling. *Cell Stem Cell*, *8*(1), 96–105. https://doi.org/10.1016/j.stem.2010.12.001

Khoei, H. H., et al. (2022). Generating human blastoids modeling blastocyst-stage embryos and implantation. *Nature Protocols*. 18, 1584–1620.

Köhler, A., Zimmerman, E., Schneider, M., Hurt, E., & Zheng, N. (2010). Structural basis for assembly and activation of the heterotetrameric SAGA histone H2B deubiquitinase module. *Cell*, *141*(4), 606–617. https://doi.org/10.1016/j.cell.2010.04.026

Kolundzic, E., Ofenbauer, A., Bulut, S. I., Uyar, B., Baytek, G., Sommermeier, A., Seelk, S., He, M., Hirsekorn, A., Vucicevic, D., Akalin, A., Diecke, S., Lacadie, S. A., & Tursun, B. (2018). FACT Sets a Barrier for Cell Fate Reprogramming in Caenorhabditis elegans and Human Cells. *Developmental Cell*, *46*(5), 611-626.e12. https://doi.org/10.1016/j.devcel.2018.07.006

Kopytova, D. V, Krasno, A. N., Orlova, A. V, Gurskiy, D. Ya., Nabirochkina, E. N., Georgieva, S. G., & Shidlovskii, Y. V. (2010). ENY2: Couple, triple...more? *Cell Cycle*, *9*(3), 479–481. https://doi.org/10.4161/cc.9.3.10610

Koutelou, E., et al. (2019). USP22 controls multiple signaling pathways that are essential for vasculature formation in the mouse placenta. *Development*. 146(4).

Lang, G., Bonnet, J., Umlauf, D., Karmodiya, K., Koffler, J., Stierle, M., Devys, D., & Tora, L. (2011). The Tightly Controlled Deubiquitination Activity of the Human SAGA Complex Differentially Modifies Distinct Gene Regulatory Elements. *Molecular and Cellular Biology*, *31*(18), 3734 LP – 3744. https://doi.org/10.1128/MCB.05231-11

Lee, K. K., Sardiu, M. E., Swanson, S. K., Gilmore, J. M., Torok, M., Grant, P. A., Florens, L., Workman, J. L., & Washburn, M. P. (2011). Combinatorial depletion analysis to assemble

the network architecture of the SAGA and ADA chromatin remodeling complexes. *Molecular Systems Biology*, *7*, 503. https://doi.org/10.1038/msb.2011.40

Leung, C. Y., & Zernicka-Goetz, M. (2015). Mapping the journey from totipotency to lineage specification in the mouse embryo. *Current Opinion in Genetics & Development*, *34*, 71–76. https://doi.org/10.1016/j.gde.2015.08.002

Li, D., Liu, J., Yang, X., Zhou, C., Guo, J., Wu, C., Qin, Y., Guo, L., He, J., Yu, S., Liu, H., Wang, X., Wu, F., Kuang, J., Hutchins, A. P., Chen, J., & Pei, D. (2017). Chromatin Accessibility Dynamics during iPSC Reprogramming. *Cell Stem Cell*, *21*(6), 819-833.e6. https://doi.org/10.1016/j.stem.2017.10.012

Li, X., Seidel, C. W., Szerszen, L. T., Lange, J. J., Workman, J. L., & Abmayr, S. M. (2017). Enzymatic modules of the SAGA chromatin-modifying complex play distinct roles in Drosophila gene expression and development. *Genes & Development*, *31*(15), 1588–1600. https://doi.org/10.1101/gad.300988.117

Li, Y., Yang, Y., Li, J., Liu, H., Chen, F., Li, B., Cui, B., & Liu, Y. (2017). USP22 drives colorectal cancer invasion and metastasis via epithelial-mesenchymal transition by activating AP4. *Oncotarget*, *8*(20), 32683–32695. https://doi.org/10.18632/oncotarget.15950

Li, Z., & Rana, T. M. (2012). A kinase inhibitor screen identifies small-molecule enhancers of reprogramming and iPS cell generation. *Nature Communications*, *3*, 1085. https://doi.org/10.1038/ncomms2059

Liao, M.-C., Muratore, C. R., Gierahn, T. M., Sullivan, S. E., Srikanth, P., De Jager, P. L., Love, J. C., & Young-Pearse, T. L. (2016). Single-Cell Detection of Secreted Aβ and sAPPα from Human IPSC-Derived Neurons and Astrocytes. *The Journal of Neuroscience: The Official Journal of the Society for Neuroscience*, *36*(5), 1730–1746. https://doi.org/10.1523/JNEUROSCI.2735-15.2016

Lin, Z., Tan, C., Qiu, Q., Kong, S., Yang, H., Zhao, F., Liu, Z., Li, J., Kong, Q., Gao, B., Barrett, T., Yang, G.-Y., Zhang, J., & Fang, D. (2015a). Ubiquitin-specific protease 22 is a deubiquitinase of CCNB1. *Cell Discovery*, *1*(1), 15028. https://doi.org/10.1038/celldisc.2015.28

Lin, Z., Tan, C., Qiu, Q., Kong, S., Yang, H., Zhao, F., Liu, Z., Li, J., Kong, Q., Gao, B., Barrett, T., Yang, G.-Y., Zhang, J., & Fang, D. (2015b). Ubiquitin-specific protease 22 is a deubiquitinase of CCNB1. *Cell Discovery*, *1*(1), 15028. https://doi.org/10.1038/celldisc.2015.28

Lin, Z., Yang, H., Kong, Q., Li, J., Lee, S.-M., Gao, B., Dong, H., Wei, J., Song, J., Zhang, D. D., & Fang, D. (2012). USP22 Antagonizes p53 Transcriptional Activation by Deubiquitinating Sirt1 to Suppress Cell Apoptosis and Is Required for Mouse Embryonic Development. *Molecular Cell*, *46*(4), 484–494. https://doi.org/https://doi.org/10.1016/j.molcel.2012.03.024

Ling, S., Li, J., Shan, Q., Dai, H., Lu, D., Wen, X., Song, P., Xie, H., Zhou, L., Liu, J., Xu, X., & Zheng, S. (2017). USP22 mediates the multidrug resistance of hepatocellular carcinoma via the SIRT1/AKT/MRP1 signaling pathway. *Molecular Oncology*, *11*(6), 682–695. https://doi.org/10.1002/1878-0261.12067

Liu, X., Vorontchikhina, M., Wang, Y.-L., Faiola, F., & Martinez, E. (2008). STAGA recruits Mediator to the MYC oncoprotein to stimulate transcription and cell proliferation. *Molecular and Cellular Biology*, *28*(1), 108–121. https://doi.org/10.1128/MCB.01402-07

Liuyang, S., Wang, G., Wang, Y., He, H., Lyu, Y., Cheng, L., Yang, Z., Guan, J., Fu, Y., Zhu, J., Zhong, X., Sun, S., Li, C., Wang, J., & Deng, H. (2023). Highly efficient and rapid generation of human pluripotent stem cells by chemical reprogramming. *Cell Stem Cell*, *30*(4), 450-459.e9. https://doi.org/10.1016/j.stem.2023.02.008

Lynch, C. J., Bernad, R., Calvo, I., Nóbrega-Pereira, S., Ruiz, S., Ibarz, N., Martinez-Val, A., Graña-Castro, O., Gómez-López, G., Andrés-León, E., Espinosa Angarica, V., del Sol, A., Ortega, S., Fernandez-Capetillo, O., Rojo, E., Munoz, J., & Serrano, M. (2018). The RNA Polymerase II Factor RPAP1 Is Critical for Mediator-Driven Transcription and Cell Identity. *Cell Reports*, *22*(2), 396–410. https://doi.org/https://doi.org/10.1016/j.celrep.2017.12.062

Ma, M. K.-W., Heath, C., Hair, A., & West, A. G. (2011). Histone Crosstalk Directed by H2B Ubiquitination Is Required for Chromatin Boundary Integrity. *PLOS Genetics*, *7*(7), e1002175. https://doi.org/10.1371/journal.pgen.1002175

Mandai, M., Watanabe, A., Kurimoto, Y., Hirami, Y., Morinaga, C., Daimon, T., Fujihara, M., Akimaru, H., Sakai, N., Shibata, Y., Terada, M., Nomiya, Y., Tanishima, S., Nakamura, M., Kamao, H., Sugita, S., Onishi, A., Ito, T., Fujita, K., … Takahashi, M. (2017). Autologous Induced Stem-Cell-Derived Retinal Cells for Macular Degeneration. *The New England Journal of Medicine*, *376*(11), 1038–1046. https://doi.org/10.1056/NEJMoa1608368

Mansour, A. A., Gafni, O., Weinberger, L., Zviran, A., Ayyash, M., Rais, Y., Krupalnik, V., Zerbib, M., Amann-Zalcenstein, D., Maza, I., Geula, S., Viukov, S., Holtzman, L., Pribluda, A., Canaani, E., Horn-Saban, S., Amit, I., Novershtern, N., & Hanna, J. H.

(2012). The H3K27 demethylase Utx regulates somatic and germ cell epigenetic reprogramming. *Nature*, *488*(7411), 409–413. https://doi.org/10.1038/nature11272

Martin, G. R. (1981). Isolation of a pluripotent cell line from early mouse embryos cultured in medium conditioned by teratocarcinoma stem cells. *Proceedings of the National Academy of Sciences of the United States of America*, *78*(12), 7634–7638. https://doi.org/10.1073/pnas.78.12.7634

McMahon, S. B., Wood, M. A., & Cole, M. D. (2000). The essential cofactor TRRAP recruits the histone acetyltransferase hGCN5 to c-Myc. *Molecular and Cellular Biology*, *20*(2), 556–562. https://doi.org/10.1128/mcb.20.2.556-562.2000

Melo-Cardenas, J., Zhang, Y., Zhang, D. D., & Fang, D. (2016). Ubiquitin-specific peptidase 22 functions and its involvement in disease. *Oncotarget*, *7*(28), 44848–44856. https://doi.org/10.18632/oncotarget.8602

Michlits, G., Hubmann, M., Wu, S. H., Vainorius, G., Budusan, E., Zhuk, S., Burkard, T. R., Novatchkova, M., Aichinger, M., Lu, Y., Reece-Hoyes, J., Nitsch, R., Schramek, D., Hoepfner, D., & Elling, U. (2017). CRISPR-UMI: Single-cell lineage tracing of pooled CRISPR-Cas9 screens. *Nature Methods*, *14*(12), 1191–1197. https://doi.org/10.1038/nmeth.4466

Mikkelsen, T. S., Hanna, J., Zhang, X., Ku, M., Wernig, M., Schorderet, P., Bernstein, B. E., Jaenisch, R., Lander, E. S., & Meissner, A. (2008). Dissecting direct reprogramming through integrative genomic analysis. *Nature*, *454*(7200), 49–55. https://doi.org/10.1038/nature07056

Miles, D. C., de Vries, N. A., Gisler, S., Lieftink, C., Akhtar, W., Gogola, E., Pawlitzky, I., Hulsman, D., Tanger, E., Koppens, M., Beijersbergen, R. L., & van Lohuizen, M. (2017). TRIM28 Is an Epigenetic Barrier to Induced Pluripotent Stem Cell Reprogramming. *STEM CELLS*, *35*(1), 147–157. https://doi.org/10.1002/stem.2453

Minkovsky, A., Patel, S., & Plath, K. (2012). Concise review: Pluripotency and the transcriptional inactivation of the female Mammalian X chromosome. *Stem Cells (Dayton, Ohio)*, *30*(1), 48–54. https://doi.org/10.1002/stem.755

Molè, M. A., Weberling, A., & Zernicka-Goetz, M. (2020). Comparative analysis of human and mouse development: From zygote to pre-gastrulation. *Current Topics in Developmental Biology*, *136*, 113–138. https://doi.org/10.1016/bs.ctdb.2019.10.002

Moraga, F., & Aquea, F. (2015). Composition of the SAGA complex in plants and its role in controlling gene expression in response to abiotic stresses. *Frontiers in Plant Science*, *6*, 865. https://doi.org/10.3389/fpls.2015.00865

Moris, N., Edri, S., Seyres, D., Kulkarni, R., Domingues, A. F., Balayo, T., Frontini, M., & Pina, C. (2018). Histone Acetyltransferase KAT2A Stabilizes Pluripotency with Control of Transcriptional Heterogeneity. *Stem Cells (Dayton, Ohio)*, *36*(12), 1828–1838. https://doi.org/10.1002/stem.2919

Mossahebi-Mohammadi, M., Quan, M., Zhang, J.-S., & Li, X. (2020). FGF Signaling Pathway: A Key Regulator of Stem Cell Pluripotency. In *Frontiers in Cell and Developmental Biology* (Vol. 8, p. 79). https://www.frontiersin.org/article/10.3389/fcell.2020.00079

Murr, R., Vaissière, T., Sawan, C., Shukla, V., & Herceg, Z. (2007). Orchestration of chromatin-based processes: mind the TRRAP. *Oncogene*, *26*(37), 5358–5372. https://doi.org/10.1038/sj.onc.1210605

Nag, N., & Dutta, S. (2020). Deubiquitination in prostate cancer progression: role of USP22. *Journal of Cancer Metastasis and Treatment*, *6*, 16. https://doi.org/10.20517/2394-4722.2020.23

Nagy, Z., & Tora, L. (2007). Distinct GCN5/PCAF-containing complexes function as co-activators and are involved in transcription factor and global histone acetylation. *Oncogene*, *26*(37), 5341–5357. https://doi.org/10.1038/sj.onc.1210604

Naryshkin, N. A., Weetall, M., Dakka, A., Narasimhan, J., Zhao, X., Feng, Z., Ling, K. K. Y., Karp, G. M., Qi, H., Woll, M. G., Chen, G., Zhang, N., Gabbeta, V., Vazirani, P., Bhattacharyya, A., Furia, B., Risher, N., Sheedy, J., Kong, R., … Metzger, F. (2014). Motor neuron disease. SMN2 splicing modifiers improve motor function and longevity in mice with spinal muscular atrophy. *Science (New York, N.Y.)*, *345*(6197), 688–693. https://doi.org/10.1126/science.1250127

Ning, B., Zhao, W., Qian, C., Liu, P., Li, Q., Li, W., & Wang, R.-F. (2017). USP26 functions as a negative regulator of cellular reprogramming by stabilising PRC1 complex components. *Nature Communications*, *8*(1), 349. https://doi.org/10.1038/s41467-017-00301-4

Oh, Y., & Jang, J. (2019). Directed Differentiation of Pluripotent Stem Cells by Transcription Factors. *Molecules and Cells*, *42*(3), 200–209. https://doi.org/10.14348/molcells.2019.2439

Ohtsuka, S., & Dalton, S. (2008). Molecular and biological properties of pluripotent embryonic stem cells. *Gene Therapy*, *15*(2), 74–81. https://doi.org/10.1038/sj.gt.3303065

Ohtsuka, S., Nakai-Futatsugi, Y., & Niwa, H. (2015). LIF signal in mouse embryonic stem cells. *JAK-STAT*, *4*(2), e1086520–e1086520. https://doi.org/10.1080/21623996.2015.1086520

Onder, T. T., Kara, N., Cherry, A., Sinha, A. U., Zhu, N., Bernt, K. M., Cahan, P., Marcarci, B. O., Unternaehrer, J., Gupta, P. B., Lander, E. S., Armstrong, S. A., & Daley, G. Q. (2012). Chromatin-modifying enzymes as modulators of reprogramming. *Nature*, *483*(7391), 598–602. https://doi.org/10.1038/nature10953

Ozyerli-Goknar, E., Kala, E. Y., Aksu, A. C., Bulut, I., Cingöz, A., Nizamuddin, S., Biniossek, M., Seker-Polat, F., Morova, T., Aztekin, C., Kung, S. H. A., Syed, H., Tuncbag, N., Gonen, M., Philpott, M., Cribbs, A. P., Acilan, C., Lack, N. A., Onder, T. T., … Bagci-Onder, T. (2022). Epigenetic-focused CRISPR/Cas9 screen identifies ASH2L as a regulator of glioblastoma cell survival. *BioRxiv*, 2022.08.17.504245. https://doi.org/10.1101/2022.08.17.504245

Papp, B., & Plath, K. (2011). Reprogramming to pluripotency: stepwise resetting of the epigenetic landscape. *Cell Research*, *21*(3), 486–501. https://doi.org/10.1038/cr.2011.28

Park, I.-H., Zhao, R., West, J. A., Yabuuchi, A., Huo, H., Ince, T. A., Lerou, P. H., Lensch, M. W., & Daley, G. Q. (2008). Reprogramming of human somatic cells to pluripotency with defined factors. *Nature*, *451*(7175), 141–146. https://doi.org/10.1038/nature06534

Pasque, V., Radzisheuskaya, A., Gillich, A., Halley-Stott, R. P., Panamarova, M., Zernicka-Goetz, M., Surani, M. A., & Silva, J. C. R. (2012). Histone variant macroH2A marks embryonic differentiation in vivo and acts as an epigenetic barrier to induced pluripotency. *Journal of Cell Science*, *125*(Pt 24), 6094–6104. https://doi.org/10.1242/jcs.113019

Pei, D., Shu, X., Gassama-Diagne, A., & Thiery, J. P. (2019). Mesenchymal-epithelial transition in development and reprogramming. *Nature Cell Biology*, *21*(1), 44–53. https://doi.org/10.1038/s41556-018-0195-z

Pengelly, A. R., Kalb, R., Finkl, K., & Müller, J. (2015). Transcriptional repression by PRC1 in the absence of H2A monoubiquitylation. *Genes & Development*, *29*(14), 1487–1492. https://doi.org/10.1101/gad.265439.115

Pfaff, N., Liebhaber, S., Möbus, S., Beh-Pajooh, A., Fiedler, J., Pfanne, A., Schambach, A., Thum, T., Cantz, T., & Moritz, T. (2017). Inhibition of miRNA-212/132 improves the reprogramming of fibroblasts into induced pluripotent stem cells by de-repressing important epigenetic remodelling factors. *Stem Cell Research*, *20*, 70–75. https://doi.org/10.1016/j.scr.2017.03.003

Qin, H., Diaz, A., Blouin, L., Lebbink, R. J., Patena, W., Tanbun, P., LeProust, E. M., McManus, M. T., Song, J. S., & Ramalho-Santos, M. (2014). Systematic identification of barriers to human iPSC generation. *Cell*, *158*(2), 449–461. https://doi.org/10.1016/j.cell.2014.05.040

Rand, T. A., Sutou, K., Tanabe, K., Jeong, D., Nomura, M., Kitaoka, F., Tomoda, E., Narita, M., Nakamura, M., Nakamura, M., Watanabe, A., Rulifson, E., Yamanaka, S., & Takahashi, K. (2018). MYC Releases Early Reprogrammed Human Cells from Proliferation Pause via Retinoblastoma Protein Inhibition. *Cell Reports*, *23*(2), 361–375. https://doi.org/10.1016/j.celrep.2018.03.057

Robinton, D. A., & Daley, G. Q. (2012). The promise of induced pluripotent stem cells in research and therapy. *Nature*, *481*(7381), 295–305. https://doi.org/10.1038/nature10761

Roedig, J., Kowald, L., Juretschke, T., Karlowitz, R., Ahangarian Abhari, B., Roedig, H., Fulda, S., Beli, P., & van Wijk, S. J. L. (2021). USP22 controls necroptosis by regulating receptor-interacting protein kinase 3 ubiquitination. *EMBO Reports*, *22*(2), e50163. https://doi.org/https://doi.org/10.15252/embr.202050163

Romito, A., & Cobellis, G. (2016). Pluripotent Stem Cells: Current Understanding and Future Directions. *Stem Cells International*, *2016*, 9451492. https://doi.org/10.1155/2016/9451492

Samara, N. L., Datta, A. B., Berndsen, C. E., Zhang, X., Yao, T., Cohen, R. E., & Wolberger, C. (2010). Structural insights into the assembly and function of the SAGA deubiquitinating module. *Science (New York, N.Y.)*, *328*(5981), 1025–1029. https://doi.org/10.1126/science.1190049

Samavarchi-Tehrani, P., Golipour, A., David, L., Sung, H., Beyer, T. A., Datti, A., Woltjen, K., Nagy, A., & Wrana, J. L. (2010). Functional Genomics Reveals a BMP-Driven Mesenchymal-to-Epithelial Transition in the Initiation of Somatic Cell Reprogramming. *Cell Stem Cell*, *7*(1), 64–77. https://doi.org/10.1016/j.stem.2010.04.015

Sawan, C., Hernandez-Vargas, H., Murr, R., Lopez, F., Vaissière, T., Ghantous, A. Y., Cuenin, C., Imbert, J., Wang, Z.-Q., Ren, B., & Herceg, Z. (2013). Histone acetyltransferase cofactor Trrap maintains self-renewal and restricts differentiation of embryonic stem cells. *Stem Cells (Dayton, Ohio)*, *31*(5), 979–991. https://doi.org/10.1002/stem.1341

Sevinç, K., Sevinç, G. G., Cavga, A. D., Philpott, M., Kelekçi, S., Can, H., Cribbs, A. P., Yıldız, A. B., Yılmaz, A., Ayar, E. S., Arabacı, D. H., Dunford, J. E., Ata, D., Sigua, L. H., Qi, J., Oppermann, U., & Onder, T. T. (2022). BRD9-containing non-canonical BAF complex maintains somatic cell transcriptome and acts as a barrier to human reprogramming. *Stem Cell Reports*, *17*(12). https://doi.org/10.1016/j.stemcr.2022.10.005

Shao, Z., Yao, C., Khodadadi-Jamayran, A., Xu, W., Townes, T. M., Crowley, M. R., & Hu, K. (2016). Reprogramming by De-bookmarking the Somatic Transcriptional Program

through Targeting of BET Bromodomains. *Cell Reports*, *16*(12), 3138–3145. https://doi.org/10.1016/j.celrep.2016.08.060

Shi, Y., Inoue, H., Wu, J. C., & Yamanaka, S. (2017). Induced pluripotent stem cell technology: a decade of progress. *Nature Reviews Drug Discovery*, *16*(2), 115–130. https://doi.org/10.1038/nrd.2016.245

Smith, K. P., Luong, M. X., & Stein, G. S. (2009). Pluripotency: Toward a gold standard for human ES and iPS cells. *Journal of Cellular Physiology*, *220*(1), 21–29. https://doi.org/https://doi.org/10.1002/jcp.21681

Soldner, F., Stelzer, Y., Shivalila, C. S., Abraham, B. J., Latourelle, J. C., Barrasa, M. I., Goldmann, J., Myers, R. H., Young, R. A., & Jaenisch, R. (2016). Parkinson-associated risk variant in distal enhancer of α-synuclein modulates target gene expression. *Nature*, *533*(7601), 95–99. https://doi.org/10.1038/nature17939

Soufi, A., Donahue, G., & Zaret, K. S. (2012). Facilitators and Impediments of the Pluripotency Reprogramming Factors' Initial Engagement with the Genome. *Cell*, *151*(5), 994–1004. https://doi.org/https://doi.org/10.1016/j.cell.2012.09.045

Stadtfeld, M., & Hochedlinger, K. (2010). Induced pluripotency: history, mechanisms, and applications. *Genes & Development*, *24*(20), 2239–2263. http://genesdev.cshlp.org/content/24/20/2239.abstract

Stegeman, R., Spreacker, P. J., Swanson, S. K., Stephenson, R., Florens, L., Washburn, M. P., & Weake, V. M. (2016). The Spliceosomal Protein SF3B5 is a Novel Component of Drosophila SAGA that Functions in Gene Expression Independent of Splicing. *Journal of Molecular Biology*, *428*(18), 3632–3649. https://doi.org/10.1016/j.jmb.2016.05.009

Strelchenko, N., Verlinsky, O., Kukharenko, V., & Verlinsky, Y. (2004). Morula-derived human embryonic stem cells. *Reproductive Biomedicine Online*, *9*(6), 623–629. https://doi.org/10.1016/s1472-6483(10)61772-5

Sun, C. (2020). The SF3b complex: splicing and beyond. *Cellular and Molecular Life Sciences*, *77*(18), 3583–3595. https://doi.org/10.1007/s00018-020-03493-z

Sun, Z.-W., & Allis, C. D. (2002). Ubiquitination of histone H2B regulates H3 methylation and gene silencing in yeast. *Nature*, *418*(6893), 104–108. https://doi.org/10.1038/nature00883

Sussman, R. T., Stanek, T. J., Esteso, P., Gearhart, J. D., Knudsen, K. E., & McMahon, S. B. (2013). The epigenetic modifier ubiquitin-specific protease 22 (USP22) regulates embryonic stem cell differentiation via transcriptional repression of sex-determining region Y-box 2 (SOX2). *Journal of Biological Chemistry*, *288*(33), 24234–24246. https://doi.org/10.1074/jbc.M113.469783

Syed, K. M., Joseph, S., Mukherjee, A., Majumder, A., Teixeira, J. M., Dutta, D., & Pillai, M. R. (2016). Histone chaperone APLF regulates induction of pluripotency in murine fibroblasts. *Journal of Cell Science*, *129*(24), 4576–4591. https://doi.org/10.1242/jcs.194035

Tada, M., Tada, T., Lefebvre, L., Barton, S. C., & Surani, M. A. (1997). Embryonic germ cells induce epigenetic reprogramming of somatic nucleus in hybrid cells. *The EMBO Journal*, *16*(21), 6510–6520. https://doi.org/10.1093/emboj/16.21.6510

Tada, M., Takahama, Y., Abe, K., Nakatsuji, N., & Tada, T. (2001). Nuclear reprogramming of somatic cells by in vitro hybridization with ES cells. *Current Biology: CB*, *11*(19), 1553–1558. https://doi.org/10.1016/s0960-9822(01)00459-6

Takahashi, K., Tanabe, K., Ohnuki, M., Narita, M., Ichisaka, T., Tomoda, K., & Yamanaka, S. (2007). Induction of Pluripotent Stem Cells from Adult Human Fibroblasts by Defined Factors. *Cell*, *131*(5), 861–872. https://doi.org/10.1016/j.cell.2007.11.019

Takahashi, K., Tanabe, K., Ohnuki, M., Narita, M., Sasaki, A., Yamamoto, M., Nakamura, M., Sutou, K., Osafune, K., & Yamanaka, S. (2014). Induction of pluripotency in human somatic cells via a transient state resembling primitive streak-like mesendoderm. *Nature Communications*, *5*, 3678. https://doi.org/10.1038/ncomms4678

Takahashi, K., & Yamanaka, S. (2006). Induction of Pluripotent Stem Cells from Mouse Embryonic and Adult Fibroblast Cultures by Defined Factors. *Cell*, *126*(4), 663–676. https://doi.org/10.1016/j.cell.2006.07.024

Takahashi, S., Kobayashi, S., & Hiratani, I. (2018). Epigenetic differences between naïve and primed pluripotent stem cells. *Cellular and Molecular Life Sciences: CMLS*, *75*(7), 1191–1203. https://doi.org/10.1007/s00018-017-2703-x

Tamburri, S., Lavarone, E., Fernández-Pérez, D., Conway, E., Zanotti, M., Manganaro, D., & Pasini, D. (2020). Histone H2AK119 Mono-Ubiquitination Is Essential for Polycomb-Mediated Transcriptional Repression. *Molecular Cell*, *77*(4), 840-856.e5. https://doi.org/https://doi.org/10.1016/j.molcel.2019.11.021

Thomson, J. A., Itskovitz-Eldor, J., Shapiro, S. S., Waknitz, M. A., Swiergiel, J. J., Marshall, V. S., & Jones, J. M. (1998). Embryonic Stem Cell Lines Derived from Human Blastocysts. *Science*, *282*(5391), 1145 LP – 1147. https://doi.org/10.1126/science.282.5391.1145

Toh, C. X. D., Chan, J. W., Chong, Z. S., Wang, H. F., Guo, H. C., Satapathy, S., Ma, D., Goh, G. Y. L., Khattar, E., Yang, L., Tergaonkar, V., Chang, Y. T., Collins, J. J., Daley, G. Q., Wee, K. B., Farran, C. A. E. L., Li, H., Lim, Y. P., Bard, F. A., & Loh, Y. H. (2016). RNAi

Reveals Phase-Specific Global Regulators of Human Somatic Cell Reprogramming. *Cell Reports*, *15*(12), 2597–2607. https://doi.org/10.1016/j.celrep.2016.05.049

Tran, K. A., Pietrzak, S. J., Zaidan, N. Z., Siahpirani, A. F., McCalla, S. G., Zhou, A. S., Iyer, G., Roy, S., & Sridharan, R. (2019). Defining Reprogramming Checkpoints from Single-Cell Analyses of Induced Pluripotency. *Cell Reports*, *27*(6), 1726-1741.e5. https://doi.org/10.1016/j.celrep.2019.04.056

Uğurlu-Çimen, D., Odluyurt, D., Sevinç, K., Özkan-Küçük, N. E., Özçimen, B., Demirtaş, D., Enüstün, E., Aztekin, C., Philpott, M., Oppermann, U., Özlü, N., & Önder, T. T. (2021). AF10 (MLLT10) prevents somatic cell reprogramming through regulation of DOT1L-mediated H3K79 methylation. *Epigenetics & Chromatin*, *14*(1), 32. https://doi.org/10.1186/s13072-021-00406-7

Ursu, A., Illich, D. J., Takemoto, Y., Porfetye, A. T., Zhang, M., Brockmeyer, A., Janning, P., Watanabe, N., Osada, H., Vetter, I. R., Ziegler, S., Schöler, H. R., & Waldmann, H. (2016). Epiblastin A Induces Reprogramming of Epiblast Stem Cells Into Embryonic Stem Cells by Inhibition of Casein Kinase 1. *Cell Chemical Biology*, *23*(4), 494–507. https://doi.org/10.1016/j.chembiol.2016.02.015

Valencia-Sánchez, M. I., De Ioannes, P., Wang, M., Vasilyev, N., Chen, R., Nudler, E., Armache, J.-P., & Armache, K.-J. (2019). Structural Basis of Dot1L Stimulation by Histone H2B Lysine 120 Ubiquitination. *Molecular Cell*, *74*(5), 1010-1019.e6. https://doi.org/10.1016/j.molcel.2019.03.029

Vallier, L., Alexander, M., & Pedersen, R. A. (2005). Activin/Nodal and FGF pathways cooperate to maintain pluripotency of human embryonic stem cells. *Journal of Cell Science*, *118*(Pt 19), 4495–4509. https://doi.org/10.1242/jcs.02553

Waddington, C. H. (1956). Genetic Assimilation of the Bithorax Phenotype. *Evolution*, *10*(1), 1–13. https://doi.org/10.2307/2406091

Wang, M., Ling, W., Xiong, C., Xie, D., Chu, X., Li, Y., Qiu, X., Li, Y., & Xiao, X. (2019). Potential Strategies for Cardiac Diseases: Lineage Reprogramming of Somatic Cells into Induced Cardiomyocytes. *Cellular Reprogramming*, *21*(2), 63–77. https://doi.org/10.1089/cell.2018.0052

Wang, T., Chen, K., Zeng, X., Yang, J., Wu, Y., Shi, X., Qin, B., Zeng, L., Esteban, M. A., Pan, G., & Pei, D. (2011). The histone demethylases Jhdm1a/1b enhance somatic cell reprogramming in a vitamin-C-dependent manner. *Cell Stem Cell*, *9*(6), 575–587. https://doi.org/10.1016/j.stem.2011.10.005

Wang, Y., Chen, S., Jiang, Q., Deng, J., Cheng, F., Lin, Y., Cheng, L., Ye, Y., Chen, X., Yao, Y., Zhang, X., Shi, G., Dai, L., Su, X., Peng, Y., & Deng, H. (2020). TFAP2C facilitates somatic cell reprogramming by inhibiting c-Myc-dependent apoptosis and promoting mesenchymal-to-epithelial transition. *Cell Death & Disease*, *11*(6), 482. https://doi.org/10.1038/s41419-020-2684-9

Wang, Y., Sun, Q., Mu, N., Sun, X., Wang, Y., Fan, S., Su, L., & Liu, X. (2020). The deubiquitinase USP22 regulates PD-L1 degradation in human cancer cells. *Cell Communication and Signaling*, *18*(1), 112. https://doi.org/10.1186/s12964-020-00612-y

Wang, Y., Zhao, C., Hou, Z., Yang, Y., Bi, Y., Wang, H., Zhang, Y., & Gao, S. (2018). Unique molecular events during reprogramming of human somatic cells to induced pluripotent stem cells (iPSCs) at naïve state. *ELife*, *7*. https://doi.org/10.7554/eLife.29518

Ware, C. B., Nelson, A. M., Mecham, B., Hesson, J., Zhou, W., Jonlin, E. C., Jimenez-Caliani, A. J., Deng, X., Cavanaugh, C., Cook, S., Tesar, P. J., Okada, J., Margaretha, L., Sperber, H., Choi, M., Blau, C. A., Treuting, P. M., Hawkins, R. D., Cirulli, V., & Ruohola-Baker, H. (2014). Derivation of naive human embryonic stem cells. *Proceedings of the National Academy of Sciences of the United States of America*, *111*(12), 4484–4489. https://doi.org/10.1073/pnas.1319738111

Wei, J., Antony, J., Meng, F., MacLean, P., Rhind, R., Laible, G., & Oback, B. (2017). KDM4B-mediated reduction of H3K9me3 and H3K36me3 levels improves somatic cell reprogramming into pluripotency. *Scientific Reports*, *7*(1), 7514. https://doi.org/10.1038/s41598-017-06569-2

Wei, Z., Gao, F., Kim, S., Yang, H., Lyu, J., An, W., Wang, K., & Lu, W. (2013). Klf4 Organizes Long-Range Chromosomal Interactions with the Oct4 Locus in Reprogramming and Pluripotency. *Cell Stem Cell*, *13*(1), 36–47. https://doi.org/https://doi.org/10.1016/j.stem.2013.05.010

Weinberger, L., Ayyash, M., Novershtern, N., & Hanna, J. H. (2016). Dynamic stem cell states: naive to primed pluripotency in rodents and humans. *Nature Reviews Molecular Cell Biology*, *17*(3), 155–169. https://doi.org/10.1038/nrm.2015.28

Wilson, M. A., Koutelou, E., Hirsch, C., Akdemir, K., Schibler, A., Barton, M. C., & Dent, S. Y. R. (2011). Ubp8 and SAGA Regulate Snf1 AMP Kinase Activity. *Molecular and Cellular Biology*, *31*(15), 3126 LP – 3135. https://doi.org/10.1128/MCB.01350-10

Worden, E. J., Hoffmann, N. A., Hicks, C. W., & Wolberger, C. (2019). Mechanism of Crosstalk between H2B Ubiquitination and H3 Methylation by Dot1L. *Cell*, *176*(6), 1490-1501.e12. https://doi.org/10.1016/j.cell.2019.02.002

Worden, E. J., Zhang, X., & Wolberger, C. (2020). Structural basis for COMPASS recognition of an H2B-ubiquitinated nucleosome. *ELife*, *9*, e53199. https://doi.org/10.7554/eLife.53199

Xiao, H., Tian, Y., Yang, Y., Hu, F., Xie, X., Mei, J., & Ding, F. (2015). USP22 acts as an oncogene by regulating the stability of cyclooxygenase-2 in non-small cell lung cancer. *Biochemical and Biophysical Research Communications*, *460*(3), 703–708. https://doi.org/https://doi.org/10.1016/j.bbrc.2015.03.093

Yagi, T., Ito, D., Okada, Y., Akamatsu, W., Nihei, Y., Yoshizaki, T., Yamanaka, S., Okano, H., & Suzuki, N. (2011). Modeling familial Alzheimer's disease with induced pluripotent stem cells. *Human Molecular Genetics*, *20*(23), 4530–4539. https://doi.org/10.1093/hmg/ddr394

Yamauchi, T., Yamauchi, J., Kuwata, T., Tamura, T., Yamashita, T., Bae, N., Westphal, H., Ozato, K., & Nakatani, Y. (2000). Distinct but overlapping roles of histone acetylase PCAF and of the closely related PCAF-B/GCN5 in mouse embryogenesis. *Proceedings of the National Academy of Sciences of the United States of America*, *97*(21), 11303–11306. https://doi.org/10.1073/pnas.97.21.11303

Yang, C. S., Chang, K. Y., & Rana, T. M. (2014). Genome-wide Functional Analysis Reveals Factors Needed at the Transition Steps of Induced Reprogramming. *Cell Reports*, *8*(2), 327–337. https://doi.org/10.1016/j.celrep.2014.07.002

Zhou, D., Liu, P., Sun, D., Chen, Z., Hu, J., Peng, S., & Liu, Y. (2017). *2785-2792-USP22-in-retinoblastoma-proliferation-aging-via-suppressing-TERT-P53-pathway.pdf*.2785–2792.

Zhu, H., Swami, S., Yang, P., Shapiro, F., & Wu, J. Y. (2020). Direct Reprogramming of Mouse Fibroblasts into Functional Osteoblasts. *Journal of Bone and Mineral Research: The Official Journal of the American Society for Bone and Mineral Research*, *35*(4), 698–713. https://doi.org/10.1002/jbmr.3929

Zhu, M., & Zernicka-Goetz, M. (2020). Principles of Self-Organization of the Mammalian Embryo. *Cell*, *183*(6), 1467–1478. https://doi.org/10.1016/j.cell.2020.11.003

Zviran, A., Mor, N., Rais, Y., Gingold, H., Peles, S., Chomsky, E., Viukov, S., Buenrostro, J. D., Scognamiglio, R., Weinberger, L., Manor, Y. S., Krupalnik, V., Zerbib, M., Hezroni, H., Jaitin, D. A., Larastiaso, D., Gilad, S., Benjamin, S., Gafni, O., … Hanna, J. H. (2019). Deterministic Somatic Cell Reprogramming Involves Continuous Transcriptional Changes Governed by Myc and Epigenetic-Driven Modules. *Cell Stem Cell*, *24*(2), 328-341.e9. https://doi.org/10.1016/j.stem.2018.11.014

Appendix 1

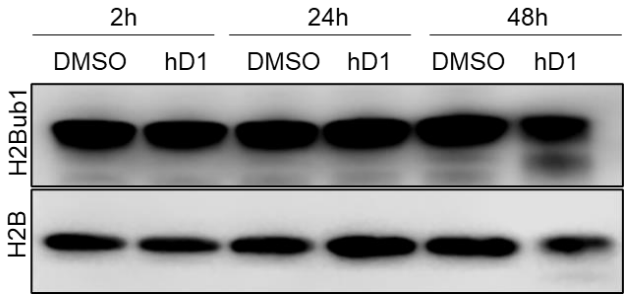

Western blot image showing H2Bub1 protein levels in HEK293T cells that was treated USP22 cyclic peptide inhibitor at different time point. H2B was used as a loading control.

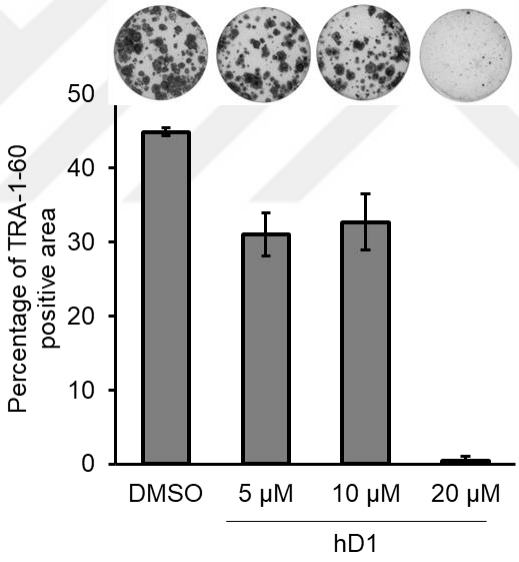

Percent area of the TRA1-60 positive cell at the end of reprogramming. Error bars indicate that technical replicates of independent n=2 biological replicates.